UNIVERSITY OF OKLAHOMA

GRADUATE COLLEGE

PHYSICAL TOPOLOGY DESIGN AND ROUTING ALGORITHMS FOR DEGREE-CONSTRAINED FSO MESH NETWORKS

A DISSERTATION

SUBMITTED TO THE GRADUATE FACULTY

in partial fulfillment of the requirements for the

Degree of

DOCTOR OF PHILOSOPHY

By

ZIPING HU
Norman, Oklahoma
2008

PHYSICAL TOPOLOGY DESIGN AND ROUTING ALGORITHMS FOR DEGREE-CONSTRAINED FSO MESH NETWORKS

A DISSERTATION APPROVED FOR THE
SCHOOL OF ELECTRICAL AND COMPUTER ENGINEERING

BY

_____
Dr. Pramode K. Verma

_____
Dr. James J. Sluss, Jr.

_____
Dr. Stamatios V. Kartalopoulos

_____
Dr. Samuel Cheng

_____
Dr. William O. Ray

.

To my husband Xiaomin Ma, my daughter SiQi Ma, and my parents

Acknowledgements

First, I would like to thank my research advisor, Professor Pramode K. Verma, for his support, encouragement, and guidance all through my graduate study.

I also would like to thank Professor Stamatios V. Kartalopoulos for his support and guidance during the first two years of my whole graduate study, and for the discussions on Chapter 4 of this dissertation. I am also grateful to Professor James J. Sluss, Jr. for his encouragement and support.

I would like to thank Professor Samuel Cheng and Professor William O. Ray for participating in both my general examination and the defense of my dissertation.

Table of Contents

Chapter 1 Introduction……1

1.1. FSO technology……..2

1.2. FSO networks……..9

1.3. Issues in FSO networks…….....11

1.4. Motivations……13

1.5. Problem statement……..15

1.6. Organization of this dissertation……16

Chapter 2 Background on Network Topology and Routing…….....17

2.1. Physical layer topology design…….....17

2.2. Routing algorithms……21

2.3. Summary……27

Chapter 3 Physical Layer Topology Design for FSO Mesh Networks…….28

3.1. Introduction……28

3.1.1. Problem statement……30

3.1.2. Previous work…….....31

3.2. Background……34

3.2.1. Delaunay Triangulation……35

3.2.2. Centralized algorithms versus distributed algorithms……..41
3.3. Physical layer topology design algorithms…….....43
3.3.1. Closest neighbor algorithm……44
3.3.2. Proposed NTD algorithm……47
3.3.3. Advantages of the NTD algorithm……..57
3.3.4. Measures of performance……60
3.3.5. Simulations and analysis……..66
3.4. Summary…….....73

Chapter 4 The NTD Algorithm in 3-dimentional Space……..74
4.1. Introduction…….....74
4.2. Review of the properties of an optimal physical topology for FSO mesh networks……75
4.3. Errors caused by the 2D-approximation of a 3D terrain……75
4.4. The 3D NTD algorithm……79

Chapter 5 Routing in FSO Mesh Networks……..82
5.1. Introduction……82
5.2. Problem statement……...86
5.3. System model……86
5.4. Mathematical background…….....89

5.5. Proposed routing algorithms…….....93

5.6. Simulations and analysis…….....108

5.7. Summary……115

Chapter 6 Conclusions……117

6.1. Achievements……117

6.2. Future work……119

References……121

Appendix…….....130

List of Tables

Table 3.1 Comparison of connectivity between CN and NTD…….67

Table 3.2 Average minimum angle comparison between CN and NTD.....71

Table 3.3 Hop count comparison between CN and NTD……72

Table 3.4 Average link length comparison between CN and NTD……73

Table 5.1.1 Average delay……..109

Table 5.1.2 Average delay……..110

Table 5.1.3 Total blocked traffic…….....111

Table 5.2.1 Average delay……..112

Table 5.2.2 Average delay……..113

Table 5.2.3 Total blocked traffic…….....114

List of Figures

Figure 1.1 A simple FSO system……3

Figure 1.2 Atmospheric attenuation for different wavelengths under clear weather conditions……5

Figure 1.3 An illustration of an FSO network deployed in metropolitan area……10

Figure 2.1 Basic physical topology structures……18

Figure 3.1 A planar graph of triangulation……36

Figure 3.2 Delaunay Triangulation……37

Figure 3.3 Edge switching……38

Figure 3.4 Special case of DT……39

Figure 3.5 A planar graph of triangulation of 30 points ……40

Figure 3.6 DT of the same 30 point set……40

Figure 3.7 40 Poisson-distributed FSO nodes……45

Figure 3.8 Network topology constructed with CN……46

Figure 3.9 Delaunay Triangulation……51

Figure 3.10 Network topology constructed with NTD……52

Figure 3.11 70 randomly distributed point-set……53

Figure 3.12 A degree-constrained minimum spanning tree……54

Figure 3.13 The constructed physical topology using CN……55

Figure 3.14 Constructed DT graph……56

Figure 3.15 Constructed graph using NTD algorithm……57

Figure 3.16 Advantage of angle enlargement in case of temporary blockage……59

Figure 3.17 Minimum pairwise degree under link failure……69

Figure 3.18 Minimum link connectivity under link failure……69

Figure 3.19 Average pairwise degree under link failure……70

Figure 3.20 Average link connectivity under link failure……70

Figure 4.1 Comparison between 2D minimum angle and 3D minimum angle……77

Figure 4.2 Relationship between a 3D angle and its corresponding 2D angle……78

Figure 5.1 A five-node network……87

Figure 5.2 A network of queues……87

Figure 5.3 Least cost path routing……97

Figure 5.4 Minimum hop count path routing……100

Figure 5.5 MHLB routing……105

Abstract

Free-space optical (FSO) mesh networks are emerging as broadband communication networks because of their high bandwidth (up to Gbps), low cost, and easy installation. However, there are two existing problems in the deployment of FSO networks: the physical topology design problem, and the routing problem. This dissertation presents an algorithm for the physical topology design of FSO mesh networks in order to enhance network reliability under defined degree constraint of each FSO node. The methodology presented enlarges the minimum angle between adjacent links at each node. Simulation results show that, compared to other methods, the proposed algorithm not only provides higher connectivity and lower delay for FSO networks, but also makes the FSO networks so constructed more tolerant in a dynamically changing environment. Further, this algorithm is enhanced to include the 3-dimensional (3-D) space, where the heights of the FSO nodes are not identical. This enhancement will apply to FSO nodes in difficult terrains where it is not feasible or desirable to have the FSO transceivers on a plane.

This dissertation also addresses the routing problem in degree-constrained free-space optical (FSO) mesh networks. To solve the routing problem, four different routing algorithms are proposed. Their performances are evaluated

through extensive simulations for a number of FSO mesh networks with different topologies and nodal degrees. The performance parameter against which these algorithms are evaluated is the mean end-to-end delay. The proposed least cost path (LCP) routing algorithm, which is based on minimizing the end-to-end delay, is considered as the bench mark. The performance of each of the other three algorithms is evaluated against the bench mark. The proposed minimum hop count with load-balancing (MHLB) routing algorithm is based on the number of hops between the source and the destination node to route the traffic. Simulation shows that the MHLB routing algorithm performs best in most cases compared with the other two. It results in minimum average delay and least blocked traffic.

Chapter 1

Introduction

Abstract: This chapter first introduces free-space optical technology for communication. Then it explains how the choices of different optical wavelengths affect the performance of optical communication when free space is the medium of transmission. Advances in the design of optical transmitters and receivers are presented. Several issues in the deployment of FSO networks are discussed.

Free-space optics (FSO) is a technology that enables communication through the air using light signals. FSO is not a new technology or invention. It has been used primarily in secure military communications for several decades. Now, it has found commercial viability driven by the following factors [1, 2]: cost effectiveness, high-bandwidth, easy deployment and redeployment. The market for FSO will increase significantly as more FSO systems are deployed and carriers become comfortable with and convinced about the reliability of FSO [3].

This chapter first introduces the design of transmitters and receivers that enable the FSO technology. FSO networks and issues in FSO networks are then addressed. Further the motivation to research topology design issues and routing problems for FSO networks is discussed.

1.1. FSO Technology

The idea of transmitting messages through the air using light signals is not new. The history of wireless optical communications can be found in [2]. Even though the idea remains relatively the same, advances in optical technology have led to a new concept called free-space optical communications. Reference [1] provides a comprehensive, unified tutorial for the readers to understand the fundamental techniques of free-space optical communications.

Free-space optical communications are emerging to meet the need of the market place because of their low cost, high bandwidth, and easy installation. An FSO communication system consists of a transmitter that transmits the modulated light signal, and a receiver at a distance that receives the signal. Figure 1.1 shows a simple FSO communication system. Reference [4] uses animations to illustrate how an FSO system works. Reference [5] presents a simulation package that allows the user to model a complete FSO system covering both the free-space propagation model and transceiver equipment

models. Reference [6] presents the authors' research on modeling of terrestrial FSO channels, modulation, and channel coding to improve the performance of FSO systems.

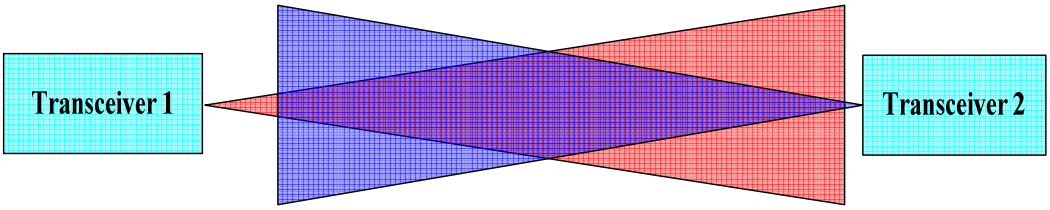

Figure 1.1 A simple FSO system

For free-space optical (FSO) communications, a narrow beam of light, which carries the information, is transmitted at a transmitting station, goes through the air, and is received at the receiving station. In-depth information can be found in reference [7] on how the laser beam propagates through the air, and how it is affected during its propagation. For most FSO systems, on-off keying (OOK) is used to modulate the light signal, where data are transmitted in a digital format with light “ON” representing a “1”, and light “OFF” representing a “0” [8]. The Pulse Position Modulation (PPM) technique is usually used in FSO systems to achieve better performance. Interested readers are referred to references [9-12] for in-depth information about this technique.

Three main factors determine the performance of an FSO system: the modulated light source from the transmitter, the detector sensitivity at the receiver, and the environment.

The modulated light source which provides the transmitted optical signal is typically a laser or light-emitting diode (LED). Transmission characteristics of an FSO communication system are partly determined by the optical wavelength chosen for the light source. Generally, all currently available FSO systems operate in the near-IR wavelength range roughly between 750 and 1600 nm, with one or two systems being developed to operate at the IR wavelength of 10,000 nm [8]. The reason for those choices of the operating wavelength range is that, even though the atmosphere is considered to be highly transparent in the visible and near-IR wavelength, certain wavelengths (or wavelength bands) suffer severe absorption when they go through the air. Figure 1.2, reproduced from reference [8], shows the absorption of the atmosphere for different wavelengths in the near-IR spectral range under clear weather conditions.

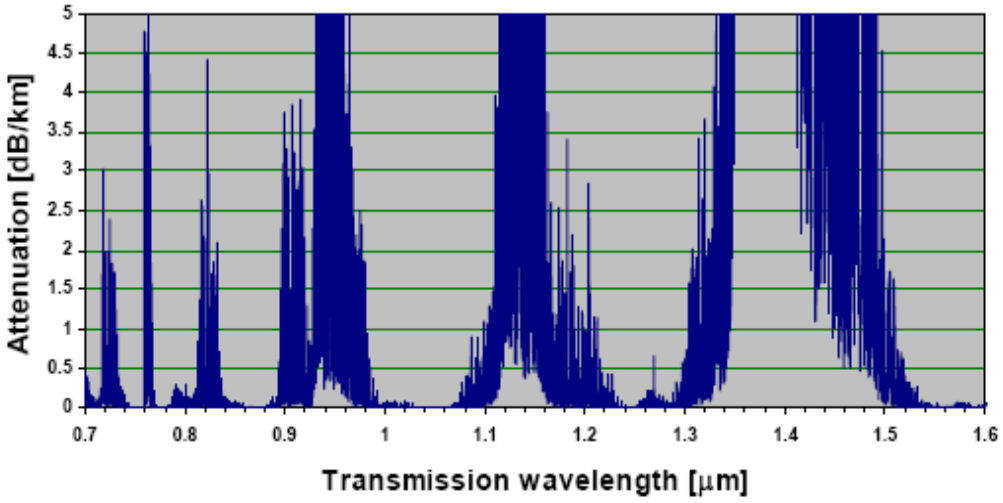

Figure 1.2 Atmospheric attenuation for different wavelengths under clear weather conditions [8]

It shows that several transmission windows are nearly transparent within the 700 to 1600 nm wavelength range, and the majority of FSO systems are designed to operate in the windows of 780-850nm and 1520-1600nm. In addition, for telecommunication purposes, lasers that are capable of being modulated at 20 Mbit/s to 2.5 Gbit/s generally can meet demands of the free-space optical communication. Lasers in the 780-925nm and 1525-1580nm spectral bands meet the frequency requirements and are available currently. To meet these requirements, Vertical Cavity Surface Emitting Lasers (VCSELs) are generally chosen for operation in the short-IR wavelength range and Fabry-Perot (FP) or distributed-feedback (DFB) lasers for operation in the longer-IR wavelength range.

The detector sensitivity also plays an important role in the overall FSO system performance. Compared with transmitters, receiver choices are much more limited. The most common material used for FSO detectors is based on silicon (Si) or indium gallium arsenide (InGaAs) technology. Germanium is another material system that covers the operating wavelength range of commercially available FSO systems. However, because of the high dark current values of this material, it is not used very often. All these materials have a broad spectral response in wavelength, and, unlike lasers, they are not tuned toward a specific wavelength; therefore, external wavelength filters must be incorporated into the receiver design in order to detect a specific wavelength. Detectors based on Si have a spectral response with maximum sensitivity around 850nm. Therefore Si detectors are ideal for use in conjunction with short-wavelength VCSELs operating at 850nm. Lower bandwidth (1-Gbit/s) Si PIN (Si-PIN) and Si APD (Si-APD) detectors are widely available. Typical sensitivity values for a Si-PIN diode are around -34dBm at 155Mbit/s. Si-APDs are far more sensitive, due to an internal amplification (avalanche) process. Therefore, Si-APD detectors are highly useful for detection in FSO systems [8]. For longer wavelength detectors, InGaAs is the most commonly used material. Commercially, most InGaAs detectors are optimized for operation at either 1310 or 1550nm. InGaAs detectors are not used in the 850nm wavelength

range because of the drastic decrease in sensitivity toward the shorter wavelength range. The majority of InGaAs receivers are based on PIN or APD technology. As with Si, InGaAs APDs are far more sensitive because of an internal amplification (avalanche) process. Sensitivity values for higher bandwidth applications can be as low as -46dBm at 155Mbit/s, or -36dBm at 1.25 Gbit/s [8].

Since both transmitter output power and receiver sensitivity are limited, reasonable power budget is important for the deployment of FSO systems. For the deployment of an FSO system, not only transmitter output power and receiver sensitivity have to be considered, but also the FSO link length because of the atmospheric attenuation and turbulence suffered when light goes through the air. The farther the light goes through the air, the more attenuation it suffers. For FSO link budget, it is also necessary to provide some system margin to compensate for product aging, misalignment, and some other factors. A survey on link budget for FSO systems can be found in [13]. Reference [14] presents the research on FSO system link budget under atmospheric turbulence.

In the current marketplace, many FSO transceiver manufacturers are competing for better quality products. FSO transceivers are being made with

smaller size, lower cost, higher reliability, easier packaging, higher efficiency, and higher bandwidth. The websites of several major FSO transceiver manufacturers can be found in [15-19]. The typical FSO transceiver specifications can also be found at these websites.

Above all, in the design of an FSO system, selecting the appropriate transmitter-receiver combination can compensate for potential shortcomings due to the use of a lower-power transmission source, and thus improve the performance of the system. Besides that, the environment also plays an important role in the performance of FSO systems. The basic requirement for an FSO system to work is Line of Sight (LOS) because light signals are directional point-to-point laser beams. Potential blockage such as buildings or trees that might block the transmission of the light signal has to be considered before the deployment of an FSO communication system. Other environmental factors that affect the performance of FSO systems include atmospheric effects, which come from the transmission media the light travels through, window attenuation, alignment or building motion, etc.

Research on mobile FSO systems is also going on. Reference [20] proposes a tracking control method for an active FSO system that enables a mobile terminal to be tracked with short range coverage. Reference [21] discusses

critical technology, architecture gaps, as well as potential approaches for the implementation of mobile FSO networks.

1.2. FSO Networks

In an FSO system, a light source is used to transmit the modulated light signal, and a detector at a distance is used to receive the signal. The design of transmitter and receiver as a matched pair makes an effective FSO system. The combination of a transmitter and a receiver is called a transceiver. A simplified FSO transceiver architecture can be found in reference [22].

An FSO node can support only a limited number of transceivers due to power, size, and weight issues. It also carries a switch or a router. Even though the pair of the transmitter and the receiver in an FSO node have separate mechanisms to transmit and receive laser beams, the transmitting and receiving can be done at the same time; therefore, an FSO transceiver is considered to work in full duplex mode. An FSO node can be easily mounted on the roof of buildings, houses, or any solid foundations.

FSO networks are emerging as broadband communication networks because of their high bandwidth (up to Gbps), low cost, and easy installation. An FSO network consists of a set of geographically distributed FSO nodes and FSO

links interconnecting the nodes. The following Figure 1.3, reproduced from reference [23], shows an FSO network deployed in a metropolitan area.

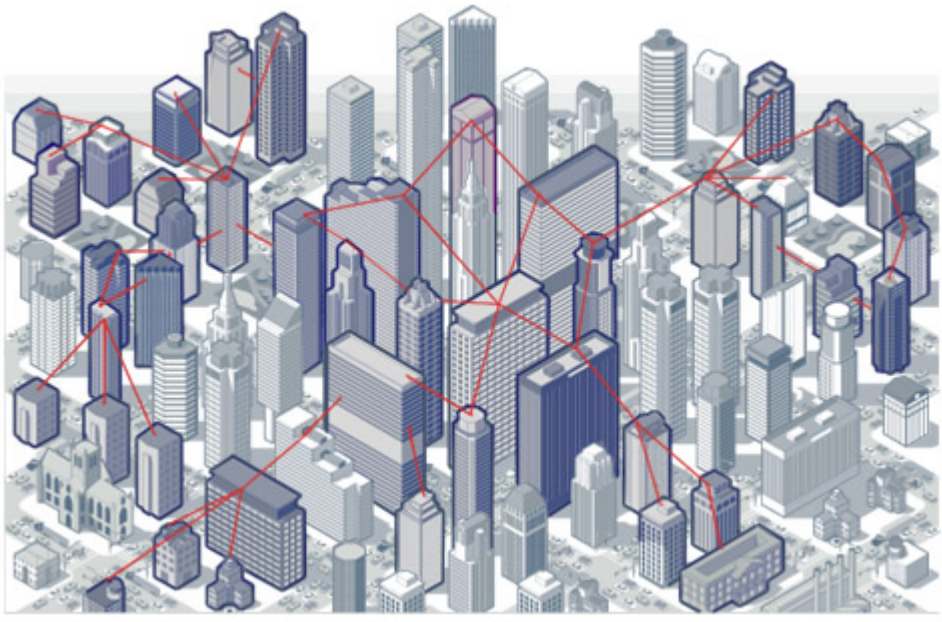

Figure 1.3 An illustration of an FSO network deployed in metropolitan area [23]

Both FSO and fiber optic transmission systems use similar infrared (IR) wavelengths of light and have similar transmission bandwidth capabilities; however, compared with fiber optical networks, FSO networks have the following advantages:

- Easy installation: the installation of an FSO node only takes less than an hour, but the deployment of fiber requires digging into the ground, which is far more time consuming and complicated. Most importantly, FSO deployment does not have any mandated licensing requirement.

- Inexpensive: the deployment of the FSO node itself is cheaper compared with the deployment of fiber because of the cost of fiber itself, the cost of digging the ground, as well as the cost of buying the necessary right of way.
- Flexibility: an FSO link can be built up or rebuilt in a different direction easily based on demands; however when a fiber is deployed, it is laid underground, and is therefore, fixed.
- Mobility: an FSO node may be moved easily based on demands; however when a fiber optic node is deployed, it has no mobility.

Therefore, FSO networks provide an attractive alternative to fiber optic networks as broadband communication networks. FSO is often referred to as “fibreless optics” or “optical wireless” transmission. Compared with wireless networks using radio frequency technology, FSO networks provide not only high capacities but also secure point-to-point transmissions. In addition, unlike RF wireless networks, FSO links are immune to electromagnetic interferences.

1.3. Issues in FSO Networks

The performance of FSO networks may be affected by various factors including environmental factors, equipment reliability, and redundancy. In this work, FSO networks with mesh architectures are dealt with. Mesh

architectures provide a high level of redundancy to match the high reliability needs of telecommunication networks.

The environmental factors affecting the performance of FSO networks include atmospheric attenuation, scintillation, window attenuation, alignment, solar interference, and line-of-sight obstructions [8]. Atmospheric attenuation is primarily dominated by fog, but can also be affected by rain, snow, dust, and various combinations of each. Atmospheric attenuations are due to absorption and scattering of atmospheric molecules and aerosols as the light beam propagates through the air. Absorption occurs when suspended water molecules and aerosols in the atmosphere extinguish photons. It leads to decreased optical power of the light signal at the receiving station, and thus the degraded performance of FSO systems. Scattering happens when the energy of the optical signal is redirected by particles along the propagation path of the light beam. Scintillation is defined as the changing of light intensities in time and space at the plane of a receiver that is detecting a signal from a transmitter located at a distance [8]. The received signal at the detector fluctuates as a result of the thermally induced changes in the index of refraction of the air along the transmission path. Thus, scintillation causes degraded performance and sometimes even results in FSO link failure. Window attenuation happens when the transmission goes through windows;

however, in many cases, window attenuation has a lesser effect on overall link availability.

Transceiver alignment is one of the key issues with FSO systems. FSO transceivers transmit highly directional narrow light beams that must impinge upon the receiver aperture of the transceiver at the opposite end of the link. The challenge is the fact that FSO receivers have a limited field of view (FOV), which can be thought of as the receiver's "cone of acceptance", and it's similar to the cone of light projected by the transmitter. For an FSO link to function, it is very important that both the transmitted beam of light and the receiver FOV cone encompass the receiver at the opposite end of the link.

Since a highly sensitive receiver in combination with a large-aperture lens is used in each transceiver for FSO signal reception, natural background light can potentially interfere with FSO signal reception. When the background radiation is associated with intense sunlight, it is called solar interference. Sometimes a FSO link fails for periods of several minutes when the sun is within the receiver's FOV [8]. Line-of sight obstructions are caused when a cloud, or a building happen to be on the propagation path of the light beam.

1.4. Motivations

Because of above mentioned issues in FSO networks, network reliability and availability are very important in the deployment of FSO networks. Availability of 99.9% or better can be achieved for well-designed FSO systems at 500m to 1km ranges. With availability of 99.5%, FSO links can go up to 2km and beyond [8]. The availability of FSO systems depends on a variety of factors, including atmospheric effects, equipment reliability, and network design (such as redundancy).

Various atmospheric effects on FSO networks have been studied in the literature and there is continuing research to improve the performance of FSO-based communication systems. Some of the research focuses on the reconfigurations of FSO networks in order to enhance the performance of FSO networks in a dynamic environment where the transmission characteristics of the free-space vary dynamically. For example, the transmitting environment changes when adverse weather conditions such as fog, heavy rain, snow, and/or heavy wind, happen. Even a portion of a cloud or a flock of flying birds may block the transmission path (or FSO link), and therefore degrade the performance of FSO networks.

Since practical algorithms for designing the physical topology of FSO networks are lacking, the focus of this dissertation is the study and development of algorithms suitable for FSO networks, which should have following properties:

- More tolerant in a dynamically changing environment and mitigating atmospheric effects as much as possible.
- No physical layer transceiver movement should be involved for network layer topology control and routing; therefore the design should have the ability to quickly cope with the changing network states.
- Achieve high path diversity, which leads to high reliability of FSO networks.
- Achieve low average delay through routing.

1.5. Problem Statement

The following two issues will be addressed in this dissertation:

Topology Design: The design of physical topologies for FSO networks deals with the problem of building the connectivity among geographically fixed FSO nodes, with a limited number of transceiver resources at each node, such that the availability of communication between any two nodes is maximized. This dissertation proposes a network topology design algorithm for building FSO mesh networks that improves their reliability.

Network Layer Routing: Based on physical layer topology and network states, network layer routing deals with the problem of finding an optimal path for

traffic between each pair of source and destination nodes that minimizes the average delay of all packets over the network. This dissertation proposes four different routing algorithms, and compares their performance with each other through extensive simulations.

1.6 Organization of this dissertation

This dissertation is organized as follows. Chapter 2 gives the background on communication network topology and routing. The proposed 2-dimentional (2-D) network topology design (NTD) algorithm and simulations are presented in Chapter 3 for physical layer topology design of FSO mesh networks. Chapter 4 presents the 3-dimensional (3-D) NTD algorithm in order to avoid errors caused by the 2D-approximation of a 3-D terrain. Chapter 5 deals with the routing problem of degree-constrained FSO mesh networks. Four different routing algorithms are proposed in order to minimize the average delay. Chapter 6 concludes the work, and provides suggestions for future work.

Chapter 2

Background on Network Topology and Routing

Abstract: This chapter introduces network topology and routing in communication networks. Different types of topologies are presented. Routing as a main function of the network layer is introduced. In particular, two popular shortest path algorithms (Dijkastra's and Bellman-Ford's algorithm) are provided.

2.1 Network topology and physical topology design

A communication network can be represented as a graph. The switches or routers are the vertices of the graph, and the communication links are the edges of the graph. A network topology is a graph consisting of a set of nodes (switches or routers) and a set of links that interconnect those nodes. It completely describes the connectivity information of a communication network. In fiber-optic communication networks, the links are optical fibers. In wireless communication networks, the links are radio frequency waves transmitted from one station to another through the air. In free-space optical communication networks, the links are narrow directional line-of-sight (LOS) laser beams. More links in a communication network typically result in higher redundancy. A

higher redundancy in a communication network results in higher reliability for the network.

For a communication network, its physical topology involves the physical (real) interconnections between nodes; whereas its logical topology involves the logical (virtual) interconnections between nodes. There are mainly five basic types of physical topologies: Ring, Bus, Star, Tree, and Mesh. Figure 2.1, reproduced from [24], shows these topologies.

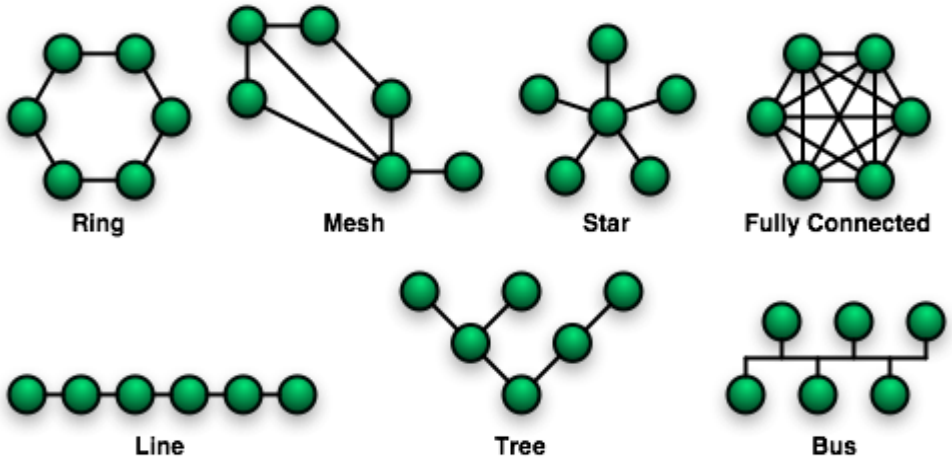

Figure 2.1 Basic physical topology structures [24]

As shown in Figure 2.1, a ring topology looks like a ring. In a ring topology, each node is connected to exactly two other nodes. At least three nodes can make a ring. Ring topologies are often used on token ring networks [25]. In a token ring network, each node has access to the token, and has the opportunity to transmit. The transmission on a token ring network is in a very

orderly fashion. The disadvantage of the ring topology is that one dysfunctional node can create problems for the entire network. Research on ring topology can be found in [26-33]. This dissertation deals with only FSO nodes each carrying at least three transceivers. Thus ring topology is not an acceptable choice; however, research on FSO networks with a ring topology can be found in reference [34].

In a bus topology, each node is connected to a central bus (using a cable as the common transmission medium). Transmission between any two nodes goes through the bus and the information is able to be received by all other nodes on the bus. Because of the propagation delay of the signal, the length of the cable is limited; therefore, a bus topology is limited in size and speed. For FSO networks, the air is the transmission medium, but, obviously it can not be used as a central bus. A bus topology is not suitable for FSO networks. Research on the bus topology can be found in [35-40].

In a star topology, each of the nodes in the network is connected to a central node with a point-to-point connection. All the data that is transmitted between two nodes is transmitted to this central node and the central node retransmits all the data to the corresponding destination node. A star topology is often used in a cable network. The main disadvantage of a star topology is that the

central node is a single point of network failure. It is not suitable for FSO networks. Research on the star topology can be found in [41-44].

A tree topology connects multiple star topologies to other star topologies. In a tree topology, there are no closed loops and there is only one path between any two nodes. For FSO networks that require high reliability, a tree topology is not a good choice because of the low connectivity it provides. Research on the tree topology can be found in [45-47].

Mesh topologies can be divided into two kinds: fully connected mesh topologies and partially connected mesh topologies (or simply mesh). In a fully connected mesh topology, each node is directly connected to each other node in the network with a point-to-point link. In a partially connected mesh topology, some of the nodes are directly connected to more than one node with a point-to-point link. Compared with other topologies, the mesh topology provides higher redundancy for communication. A fully connected mesh topology has the highest redundancy. However, because of the degree constraint of each FSO node (each node can support only a limited number of transceivers); it is often not possible to build a fully connected mesh topology. This dissertation is focused on building a partially connected FSO mesh network with high connectivity using innovative choices in physical topology and routing.

Physical layer topology design of a communication network is a blueprint for building the network. Physical layer topology design involves specifying the locations of the nodes and the interconnections between the nodes through communication links such as cables or optical fibers, or wireless links, such as FSO and RF. Since this work focuses on FSO networks, only the locations of nodes and placement of the number and directionality of optical transceivers at each node are the primary consideration in FSO network topology design.

For physical topology design of FSO mesh networks, the FSO link failure probability has to be taken into consideration because FSO links are subject to the various environmental factors such as fog, rain, scintillation, LOS blockage, etc. The work described in this dissertation focuses on improving the reliability of FSO mesh networks in a dynamically changing environment.

2.2 Routing algorithms

In this dissertation, an FSO network consisting of FSO nodes and links between the nodes is treated as an autonomous system [48].

In a packet switching network, packets are forwarded from router to router on a path from the source node to the destination node. For a router to perform its

function, it must have information about the network topology and the best route to follow. The routing decision is based on the routing algorithm. The routing algorithm is that part of the network layer software responsible for deciding the output line to which an incoming packet would be directed [49]. The routing algorithm is usually designed based on some form of least-cost criterion. The criterion might be based on minimizing the number of hops between the source-destination node pairs, minimizing the utilization factor associated with links, or some combination of the two. Additionally, minimization of end-to-end delay is another important criterion that drives the routing algorithm. Maximization of network throughput is another criterion that can be the basis for the design of a routing algorithm.

There are two types of routing algorithms: static routing algorithms and adaptive routing algorithms. For static routing algorithms, the routing decisions are made not based on current traffic and network topology, but calculated in advance, off-line, and downloaded to the routers when the network is booted. For adaptive algorithms, the routing decisions are made based on changes in the network topology, and usually the traffic. Modern communication networks generally use adaptive routing algorithms rather than static ones because static routing algorithms do not take the current network state into consideration.

Two adaptive routing algorithms are the most popular: distance vector routing and link state routing [48]. Distance vector routing requires that each node exchange information with its neighboring nodes. Two nodes are said to be neighbors if both of them are directly connected to the same network. Distance vector routing operates by maintaining a routing table at each router that contains the best known distance to each destination and which link to use to get there. These routing tables are updated by exchanging information with the neighboring nodes. In the routing table of each router, each entry contains information including the preferred outgoing line to get to the destination, and an estimated time or distance to that destination. The metric used might be number of hops; time delay in milliseconds, total number of packets queued along the path, etc.

The other adaptive routing algorithm is called link state routing. Variants of link state routing are now widely used. Using link state routing, each router operates according to the following five steps [50]:

1. Discover its neighbors and learn their network addresses.
2. Measure the delay or cost to each of its neighbors
3. Construct a packet telling all it has just learned.
4. Send this packet to all other routers.

5. Compute the shortest path to every other router.

In effect, the complete topology and all delays are experimentally measured and distributed to every router. Then, a shortest path algorithm is run to find the shortest path to every other router.

Variants of Dijkstra's [51], [52], or Bellman-Ford's [53] algorithm are most widely used in both static routing and adaptive routing algorithms to find the shortest path between a pair of source-destination nodes. If the network topology and link cost information are given, Dijkastra's algorithm can be stated as follows: Find the shortest paths from a given source node (or vertex) to each other node (or vertex) by developing the path in order of increasing path length. The algorithm proceeds in stages [48]. Initially, the source node is put in a set T, and all the initial costs from the source node to all neighboring nodes are calculated. Then at the first stage, the least cost path from the source node to its neighboring node is determined, and the node that is closest to the source node is put in the set T. By the k^{th} stage, the shortest paths to the k nodes closest to the source node have been found; these nodes are included in the set T. At stage k+1, the node not in T that has the shortest path from the source node is added to T and its path from the source is also included. Dijkstra's algorithm can also be described in detail as follows. For an N nodes

network, to find the shortest paths from a source node s to each of the other nodes in the network, first define

T = set of nodes found at different stages by the algorithm

Tree = spanning tree for the nodes in T that includes links that are on the least-cost paths from s to each node in T

w(i, j) = link cost (or weight) from node i to node j; if two nodes are directly connected, then $w(i, j) \geq 0$; otherwise, $w(i, j) = \infty$.

L(n) = cost of the least-cost path from node s to node n that is found by the algorithm.

The algorithm operates according to the following 3 steps. Steps 2 and 3 are repeated until T = N, which means that the shortest paths from node s to each of the other nodes are found.

Step 1: T = Tree = [1]; L(n) = w(s, n) for $n \neq s$

Step 2: Suppose j represents all the neighboring nodes not in T, then there exists a neighboring node x such that

For $x \notin T$, L(x) = min L (j)

Step 3: For all $n \notin T$, L(n) = min [L(n), L(x) + w(x, n)]

The algorithm terminates when all nodes are added to the set T. The spanning tree T presents all the least-cost (or shortest) paths from source node s to each of the other nodes in the network.

Bellman-Ford's algorithm [48] uses a different approach to find the shortest path from a source node to the destination node. It assumes that the network topology and link cost information are given. For an N nodes network, to find all the shortest paths from source node s to each of the other nodes in the network, it defines,

w(i, j) = link cost (or weight) from node i to node j; if two nodes are directly connected, then $w(i, j) \geq 0$; otherwise, $w(i, j) = \infty$.

h = maximum number of links in a path at the current stage of the algorithm

$L_h(n)$ = cost of the least-cost path from node s to node n under the constraint of no more than h links

The Bellman-Ford algorithm operates according to the following two steps. Step 2 is repeated until none of the costs changes:

Step 1: $L_0(n) = \infty$, for all $n \neq s$

$L_h(s) = 0$, for all h

Step 2: For each successive $h \geq 0$, and each $n \neq s$, compute

$$L_{h+1}(n) = \min_{j} [L_h(j) + w(j, n)] \qquad j \text{ is the predecessor node of node } n$$

The algorithm first finds the shortest paths from a given source node s under the constraint of that the paths contain at most one link. Then it finds the shortest paths that contain at most two links. In this way, the algorithm progresses until the shortest paths from the source node s to each other node have been found, and no changes can be made.

2.3 Summary

This chapter has given an introduction to the physical topology and routing of a communication network. It has presented several basic physical topologies of communication networks. It has also reviewed two popular shortest path algorithms that are widely used for routing. Based on this knowledge, the following four chapters present the basis and outcome of research reported in this dissertation.

Chapter 3

Physical Layer Topology Design for FSO Mesh Networks

Abstract: This chapter proposes a method for the physical topology design of free-space optical (FSO) mesh networks in order to enhance network reliability under defined degree constraint of each FSO node. The methodology presented in this chapter enlarges the minimum angle between adjacent links at each node. Simulation results show that, compared to other methods, the proposed algorithm not only provides higher connectivity and lower delay for FSO networks, but also makes the constructed FSO networks more tolerant in a dynamically changing environment.

3.1 Introduction

Free-space optical (FSO) networks are emerging as broadband communication networks by providing high data rate (up to Gbps), low cost, and secure physical layer point-to-point directional laser beam transmissions. Those directional laser beams form communication links among FSO nodes. FSO nodes are portable, inexpensive, and easy to install. They can be distributed over a large geographical area. An FSO node mainly consists of a switch (or a router) and several transceivers. Each transceiver is able to track the incoming

photonic signal from a transceiver in another FSO node. An FSO node can carry only limited number of transceivers due to size, weight and power issues. FSO networks consist of FSO nodes and FSO links interconnecting the nodes. In this chapter, it is assumed that all FSO nodes in an FSO network are identical, and the FSO node operates in a full-duplex mode.

Physical layer connections (or links) can be built among FSO nodes through tracking and acquisition processes. The narrow beam of light (FSO link) has small beam divergence that allows for secure and efficient transmission with a major fraction of the transmitted power being collected by the receiver. FSO receivers have a limited field of view (FOV) of only a few degrees, which can be considered as their “cone of acceptance”, similar to the cone of light projected by the transmitter. All of these lead to low latency for forming an FSO link; therefore building and maintaining an optimal physical layer topology that endures a relatively long time are very important for FSO networks.

FSO links may suffer from a high probability of failure because of various atmospheric effects and changes in the environment. For example, FSO link without redundancy may fail during the whole daytime for several days because of atmospheric scintillations. A vivid example is given in [50]. The performance of FSO networks may be further degraded because of a high

probability of dependency of link failure events when FSO links are geographically close to each other. For example, two FSO links that have geographic proximity have a high probability of both suffering from link failure during the same time due to heavy fog.

To improve the reliability of an FSO mesh network through topology design, it is necessary to increase the spatial diversity of FSO links in order to decrease the dependency of link failure events. In addition, in order to mitigate the effect of FSO link failure on an FSO network, it is also necessary to increase the path diversity (or multi-path disjointedness) between a source node and the corresponding destination node in the FSO mesh network. Mesh architecture is a good choice of network topology for FSO networks in a dynamically changing environment by providing high redundancy [54, 55].

In this chapter, the topology design problem for a FSO mesh network is first presented. Then previous research on physical topology design is introduced, especially the Closest Neighbor (CN) algorithm. At last, the proposed topology design algorithm is presented, and compared with the CN algorithm through extensive simulation.

3.1.1 Problem statement

Consider FSO nodes as a set of points; an FSO link based mesh topology consisting of FSO nodes and FSO links interconnecting them is treated as a graph G(V, E). FSO nodes are taken as vertices V of the graph. FSO links are taken as edges E of the graph. The general problem of physical layer topology design for FSO networks is formulated as follows.

Given a set of randomly distributed FSO nodes with a defined degree constraint, find a topology design algorithm that provides high connectivity (or reliability) for the resulting FSO network.

3.1.2 Previous work

That the performances of FSO systems can be greatly degraded in a dynamically changing environment has been introduced in Chapter 1. The primary factors affecting performance include atmospheric attenuation, scintillation, window attenuation, alignment or building motion, solar interference, and line-of-sight obstruction. All these factors affect both the reliability and the availability of FSO systems.

Performance degradation due to atmospheric effects on FSO systems are reported in [8, 56-59]. Reference [56] presents authors' research on feasible study of FSO links under atmospheric turbulence. Detailed analysis is shown in

[7] on absorption and scattering process when laser beam goes through the air. The effects of fog on visibility and range at different locations are reported in [8] in detail. The bit-error-rate (BER) of an FSO system increases greatly when there is atmospheric scintillation. Investigations on the performance of FSO systems under atmospheric scintillation have been done in [59]. Solar interference may cause an FSO link to fail for several minutes during a normal sunny day [8]. The line-of-sight (LOS) obstruction is another problem that affects FSO systems. When an FSO link is to be built, the surrounding area also needs to be considered. For example, there should not be growing trees or buildings in the path of the FSO link, otherwise, the link might be blocked. An FSO link may also be temporarily blocked by a piece of passing cloud or a flock of flying birds.

The reliability (or availability) of FSO networks is not only affected by the above mentioned factors, but also affected by two other factors: equipment reliability and network design. Research has been done to improve the reliability of FSO networks through different approaches. The reliability of different FSO systems under different weather conditions is evaluated through experiments in [57].

To compensate for atmospheric effects on FSO systems, spatial diversity can be employed, which is shown in [7]. An adaptive transceiver architecture is

proposed in [60] to provide flexibility and agile operation of transceivers in a dynamic environment. The proposed adaptive terminal is capable of changing rate and modulation format in order to improve overall availability under changing link conditions. A simple approach is proposed and experimentally demonstrated in [61] for scintillation suppression of FSO channels using saturated optical amplifiers. To compensate for the disadvantage of FSO systems under changing link conditions, a hybrid RF/FSO architecture is proposed in [62] which increases the availability of FSO networks. Through error analysis of multi-hop FSO communication systems in [63], the authors argue that the reliability of a FSO link is improved by application of specific coding schemes.

The improvement of reliability of FSO networks can also be achieved through network design. Research in [34] focuses on dynamic reconfiguration of FSO networks through topology control to achieve minimum congestion. Their work is limited to two transceivers per FSO node. Through topology control, reference [64] claims that obscuration in FSO networks can be minimized. Reference [65] presents a technique that leads to multi-objective optimization in FSO networks through topology control. However, all the above mentioned research needs the reconfiguration of FSO networks, which is time-consuming because it involves the realignment of transceivers; therefore, these schemes

are not practical. Research in [66] proposes a novel topology control algorithm (NTC) for packet radio networks to achieve high connectivity and throughput. A distributed topology design algorithm is proposed in [67] with the main purpose of “fast connectivity” for military applications without considering other performance parameters (such as redundancy, system margin) of FSO networks. Three topology design algorithms are proposed in [68] focusing on increasing the connectivity of FSO networks, which is similar to our approach. They are modified Delaunay Triangulation (MDT), Closest Neighbor (CN), and farthest neighbor (FN) algorithms. Among them the CN algorithm starting from constructing a degree-constrained minimum spanning tree (DCMST) has been proven to outperform the others.

To improve the reliability of FSO networks under dynamically varying transmission environments, redundant links are necessary. Mesh topology is a good choice for FSO network architecture due to the redundancy it can provide. However, the number of transceivers at each FSO node (or the maximum degree of each node) is limited. Design of a degree-constrained topology is NP-complete [68]. Heuristic approaches need to be used to solve the problem.

3.2 Background

The proposed topology design method involves a basic data structure in computational geometry: Delaunay Triangulation (DT). An introduction of DT is given next. Interested readers are referred to [69] for an in-depth understanding. In this section, two different types of algorithms are compared for physical topology design of FSO networks: centralized algorithms and distributed algorithms.

3.2.1 Delaunay Triangulation

As observed before, the probability of FSO link failure is very high in a dynamically changing environment. A shorter FSO link therefore provides better performance. A physical topology with local connections thus provides a higher reliability. The proposed algorithm starts with a planar graph that has the maximum number of edges. A planar graph is a graph within which no two edges cross each other. A planar graph with maximum number of edges is a triangulation, i.e., a graph inside which all bounded regions are triangles [70]. There are two reasons for the algorithm starting with building a planar graph of triangulation: first, most of the edges in a planar graph of triangulation are local connections; therefore, the lengths of most FSO links are relatively short. Second, a planar graph of triangulation provides high redundancy, and high redundancy leads to high reliability.

Figure 3.1 shows a planar graph of triangulation for a 10 point-set.

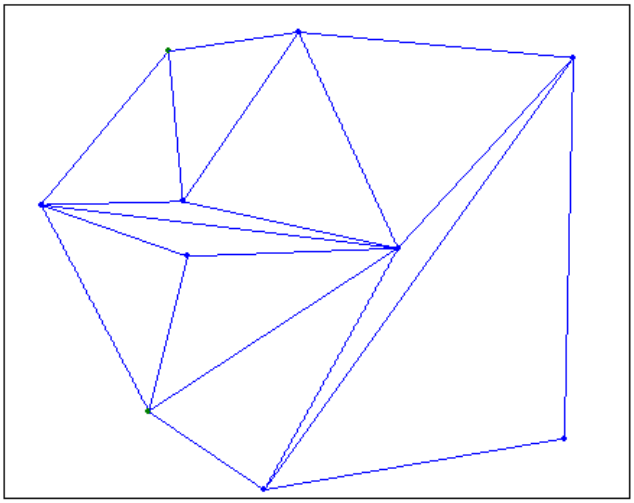

Figure 3.1 A planar graph of triangulation

Intuitively, it is desirable to have links in all directions at a node in order to have a good forward progress for a transit packet [70]. One way to do that is to maximize the minimum angle of all triangles in the planar graph of triangulation (MAX-MIN criterion). A Delaunay triangulation (DT) over a set of points is the result of the MAX-MIN operation. Therefore, Delaunay Triangulation is a unique planar graph of triangulation that has the maximum minimum angle among the angles of all the triangles [69]. Figure 3.2 shows the DT formed with the same 10 point set.

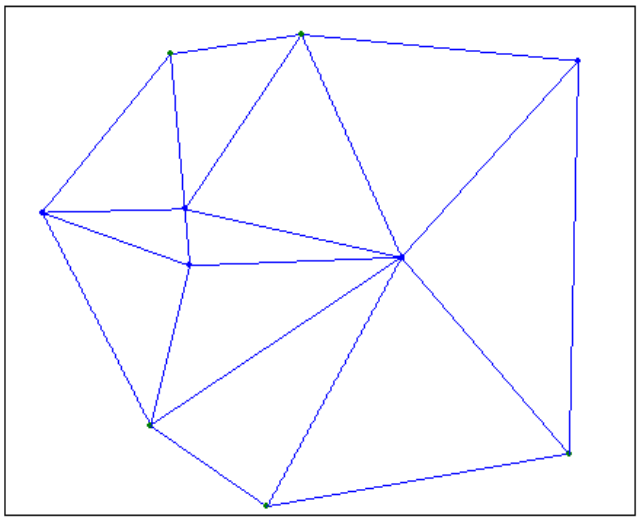

Figure 3.2 Delaunay Triangulation

Construction of the DT of a given point set is the first step in the process. There are three main reasons for that:

- DT is a unique planar graph of triangulation that has the maximum minimum angle. Since FSO links are subject to atmospheric effects, a larger angle among adjacent links will better mitigate degradation caused by atmospheric effects.
- Since DT is a planar graph of triangulation, which has maximum number of edges among all planar graphs, it has high redundancy, and it is more difficult to disconnect a DT by removing a few edges or nodes.

- Since DT is a planar graph of triangulation, most of the edges in a DT are connections among nodes close to each other [70]; therefore, most edges are likely to be short edges. Compared with FSO links (or edges) of longer length, shorter FSO links have a higher system margin, leading to better performance.

One way to construct Delaunay Triangulation is through edge switching (or flipping) [69]. For a given point set, first find a planar graph of triangulation; then for any two adjacent triangles, switch their shared edge if the operation can maximize their minimum angle; repeat until the minimum angle in the graph is maximized. The final formed graph is a unique DT. For example, Figure 3.3 (a) shows two adjacent triangles in a planar graph of triangulation. By performing an edge switching on their shared edge, the minimum angle in the graph is maximized. Figure 3.3 (b) shows the graph after edge switching.

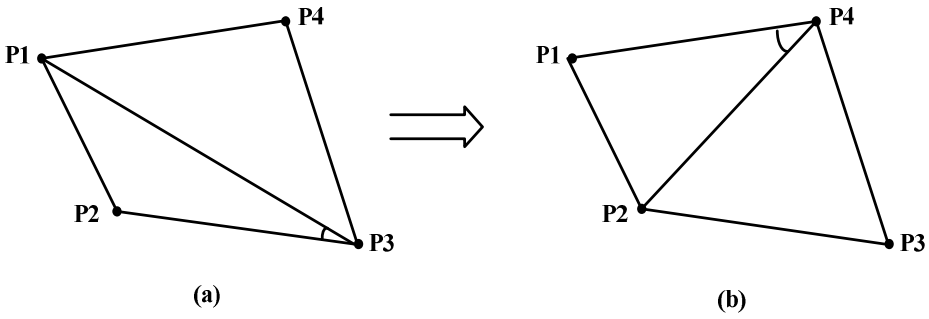

Figure 3.3 Edge switching

Besides the Maximum Minimum Angle property, DT has another property called the Empty Circle property. The empty circle property states that any three vertices that form a triangle in a DT lie on the circumcircle of the triangle, no point of a DT lies inside the circumcircle. In a special case, there might be four points of two adjacent triangles that lie on the same empty circle. In this case, for any two adjacent triangles formed by these four points, the minimum angle is the same. Figure 3.4 shows the case.

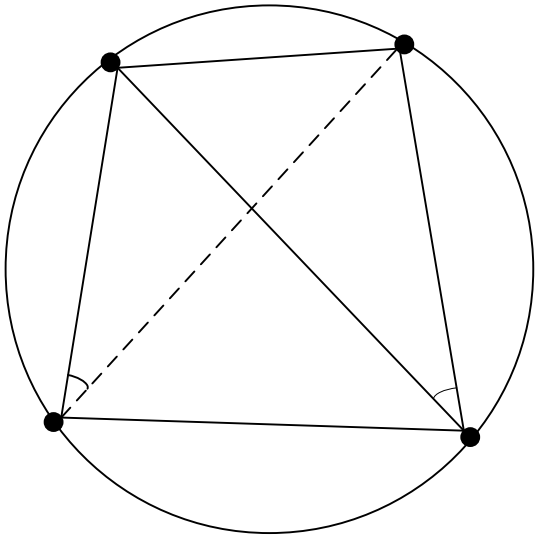

Figure 3.4 Special case of DT

In this special case, the shared edge is chosen as the one of shorter length because FSO links of shorter length have higher system margin. Similarly, when there are more than four points that lie on the same circumcircle, the

shared edges are added in to the graph of triangulation in ascending order of their length.

The following Figure 3.5 illustrates a planar graph of triangulation of 30 points. After the edge switching operation, Figure 3.6 illustrates the Delaunay Triangulation formed over the same point set.

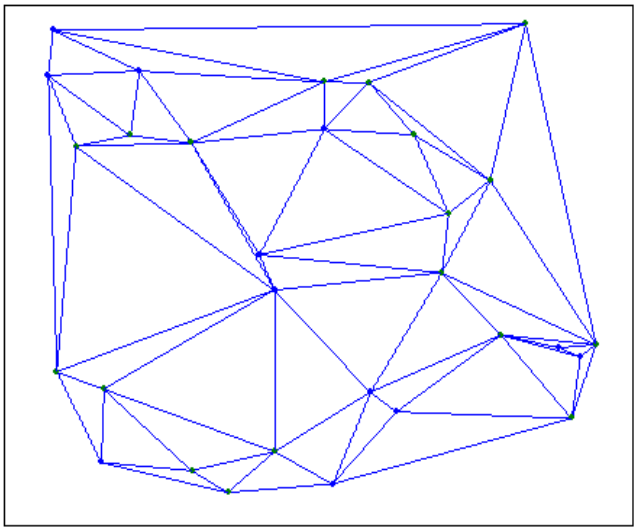

Figure 3.5 A planar graph of triangulation of 30 points

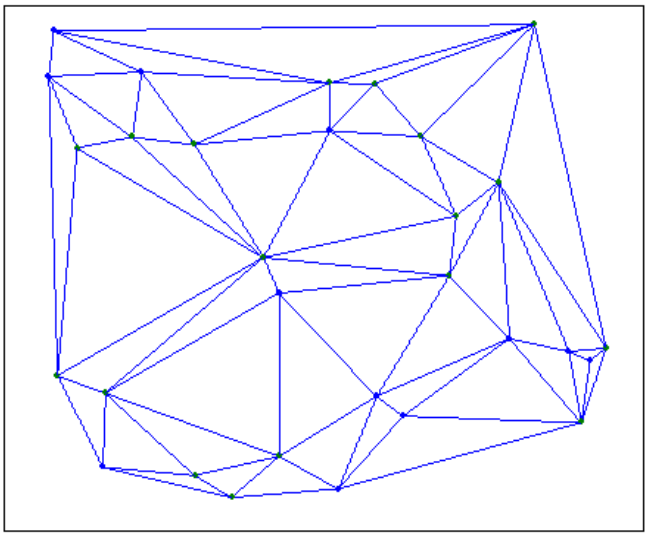

Figure 3.6 DT of the same 30 point set

Delaunay Triangulation finds applications in different areas such as sensor networks, communications, signal processing, multimedia, micromechanics, etc, [71-78].

3.2.2 Centralized algorithms versus. Distributed algorithms

To form physical layer connections of an FSO network with degree constraint at each node, both centralized and distributed topology design algorithms may be used. A distributed algorithm is proposed in [67]. Several centralized algorithms are proposed in [68]. Comparing a distributed algorithm with a centralized algorithm, the distributed algorithm has following disadvantages:

- In a distributed algorithm, the decision to form links at each node is made locally without global knowledge of the distribution of all FSO nodes; therefore, the final formed topology is not optimal which leads to poor performance (such as low redundancy) of FSO networks.
- The execution of the distributed algorithm takes a number of rounds. At each round, several transceivers with auto-tracking function simultaneously change their respective directions independently to establish FSO links with other nodes. Therefore, the total time involved is equal to the number of rounds taken to execute the algorithm times the time used for the physical movement of a transceiver [67]. The movement of a transceiver (only for alignment purposes) takes about 500 milliseconds. Therefore, the deployment of the distributed algorithm is complicated and time consuming.
- A FSO transceiver transmits a highly directional narrow light beam that must impinge upon the receiver aperture of the transceiver at the opposite end of the link [8]. Thus FSO link alignment is a big issue in the deployment of FSO networks. The farther the distance, the harder the link alignment is. The deployment of the distributed algorithm involves much more link alignments than for a centralized algorithm. Therefore, the distributed algorithm is not practical for physical layer topology design of FSO networks.

- As stated in [67], the execution of the distributed algorithm requires synchronization among FSO nodes. No solution is proposed currently.
- During the deployment of distributed topology design algorithm, a lot of communication and exchange of control information needs to be done among FSO nodes. Therefore, communication complexity is increased.

Compared with the distributed algorithm, the deployment of a centralized algorithm requires a centralized node or a central network processor to run the algorithm assuming that the location of each FSO node is known. All locations of FSO nodes can be obtained using GPS (Global Positioning System) devices. A mechanism is needed to collect information of all nodal locations and to distribute the calculated topology (or graph) to all nodes. However, the centralized algorithm has following advantages:

- It is simple. Only a centralized node or a central network processor is involved in the execution of the algorithm.
- The deployment of a centralized algorithm for the physical layer connections of a FSO network requires only one movement for each transceiver; it is easy and also time-saving.
- For the deployment of a centralized algorithm, no communication and exchange of control information is needed among FSO nodes; therefore, communication complexity is low.

- No synchronization among FSO nodes is needed for the execution of a centralized algorithm.

Based on the above discussions, in the proposed approach, a centralized algorithm is chosen for the topology design of FSO mesh networks.

3.3 Physical layer topology design algorithms

In this section, a recent study on topology design of FSO mesh networks is presented first. Then, the proposed topology design method is provided. Through extensive simulation, it is shown that the proposed topology design algorithm achieves better performance.

3.3.1 Closest Neighbor (CN) algorithm

It is known that an FSO node can support only a limited number of transceivers; therefore, the number of links formed at that node is limited. The degree of an FSO node is equal to the number of FSO links interconnecting it with other nodes. In other words, the maximum degree of an FSO node is equal to the number of transceivers it carries. To solve the physical topology design problem of degree-constrained FSO mesh networks, several approaches have been proposed in [68]. Among them, the Closest Neighbor (CN) algorithm outperforms the others. In this section, the CN algorithm is

briefly introduced. Interested readers are referred to [68] for in-depth information.

Given a set of FSO nodes, the CN algorithm starts from constructing a degree-constrained Minimum Spanning Tree (DCMST). According to [68], the DCMST graph is built to guarantee the connectivity of the network, which means that between each pair of source-destination nodes, one path is guaranteed to exist. The DCMST is constructed according to the algorithm proposed in [79]. Then, assuming that the degree constraint of each node is Δ, nodes with degree less than Δ are picked in the increasing order of their current degree δ. Starting from the node with minimum δ, each node is connected with its Δ - δ closest neighbors. In this scheme, after forming DCMST, at the next stage, shorter links have higher priority of being added to the graph without violating the degree constraint. It can be seen from the following example that in the final graph, most connections are formed locally.

As an example, 40 FSO nodes which are Poisson-distributed in a 40×40 square are shown in Figure 3.7. Assuming that the degree constraint Δ of each FSO node is 4, the final topology constructed using the CN algorithm is shown in Figure 3.8.

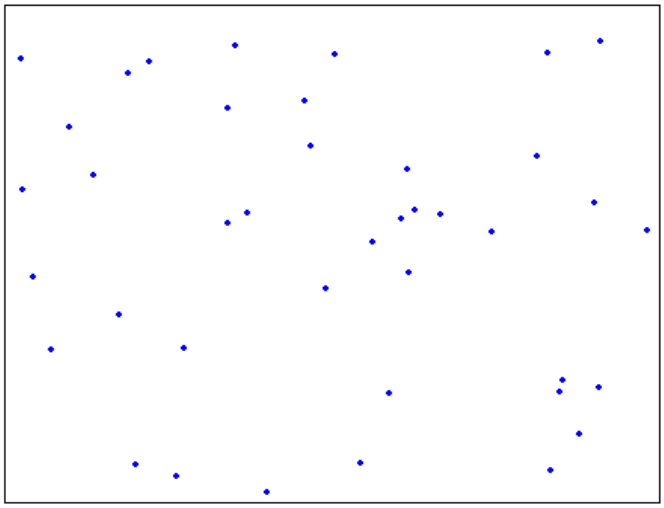

Figure 3.7 40 Poisson-distributed FSO nodes

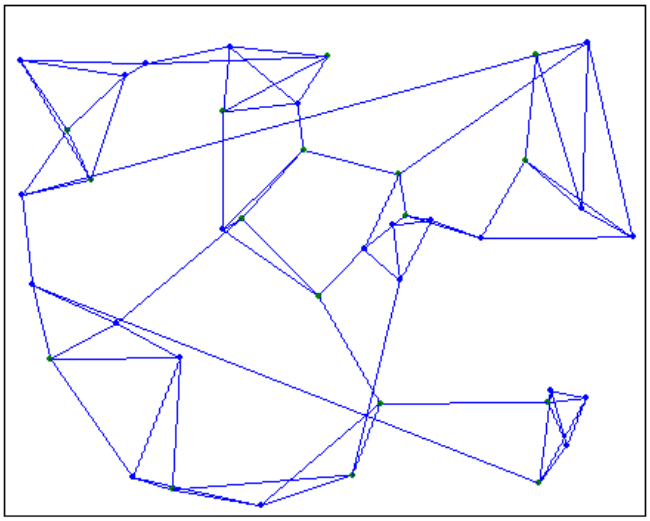

Figure 3.8 Network topology constructed with CN

It is reasonable to think that the topology (or graph) should be constructed by connecting each FSO node to its closest neighboring nodes as in the CN algorithm. Besides that, by forming the DCMST as a first step, it is guaranteed that there exists at least one path between each source-destination node pair. However, to achieve high reliability; the graph should also have the property that it should be difficult to disconnect the graph by removing a few edges or nodes. Since most links are local connections, as shown in Figure 3.7, the graph constructed with the CN is not promising. In addition, in order to mitigate atmospheric effects on FSO networks, adjacent FSO links at a node should diverge in different directions with as wide an angle between them as possible. Since atmospheric effects are often localized, divergence of the angle between adjacent links at a node provides a higher probability of having a functional redundant link.

Based on above analysis, the following properties for the topological design of a mesh FSO network can be specified.

- FSO links at any node should have high angular divergence, which also implies high spatial diversity.
- It should be difficult to disconnect an FSO network by removing a few links or nodes.

- Although all links are assumed to be within the allowable transmission range, shorter FSO links have higher system margin; therefore, in the topology design of FSO networks, nearer nodes should have a higher priority of being connected to a given node.

3.3.2 The Proposed NTD algorithm

The proposed network topology design scheme described in this section is the extension of the work of both [66] and [68]. A Delaunay Triangulation (DT) graph is used as a starting point in both NTC [66] and MDT [68] algorithms. Although NTC may result in good topology for packet radio networks, it is not suitable for FSO networks with high probability of link failure. Using the MDT algorithm, after forming a DT, edges are removed and added at following steps mainly to satisfy the degree constraint of FSO networks. Their simulation results show that the MDT is not as good as their proposed CN algorithm. In the proposed approach, after forming the Delaunay Triangulation of a given point set, edges have to be removed from the DT graph in order to satisfy the degree constraint of the network. During the process, the longer edge of two adjacent edges that forms the minimum angle at the node violating the given degree constraint are removed intentionally. The process is repeated until the degree constraint at each node is satisfied. As a result, in the network constructed with the proposed algorithm, the minimum angle at each node is

enlarged. This angle enlargement strategy is used to increase the spatial diversity of FSO links. Through extensive simulations, it is shown that FSO networks constructed with the proposed network topology design (NTD) algorithm achieve not only high spatial diversity, but also high reliability. This work considers only cases with at least three transceivers per FSO node.

The following assumptions are made first.

- All FSO nodes' locations are known.
- The lengths of all FSO links are within the allowable transmission range.
- Each FSO node has the same degree constraint Δ.
- Through a tracking and acquisition process, each node is able to build point-to-point optical links in any direction with other nodes.

Given a set of nodes and the information of their locations, the proposed network topology design (NTD) algorithm follows.

Step 1: Construct the DT of the given set of nodes.

Step 2: For nodes with degree higher than Δ in the DT, remove the longer edge of two adjacent edges that form the minimum angle. Repeat until the degree constraint of each node is met.

Step 3: For nodes with degree less than Δ, edges are added in ascending order of their lengths without violating the degree constraint at any node.

A pseudo-code of the algorithm is described as follows:

*/ * Pseudo Code for the Proposed NTD Algorithm */*

```
/*Input: a set of points (or nodes) with location information */
/*Output: a graph (or topology) constructed with NTD algorithm */
NTD( )
{
 /* Step 1: construct Delaunay Triangulation */
 Delaunay_Triangulation( ); /* start constructing graph G of Delaunay Triangulation of the input point set */

/* Step 2: edge_deleting */
max_deg = find_max_deg( ); /* find the maximum nodal degree in graph G */
while(max_deg > Δ) {
        find_min_angle( ); /*Find the minimum angle between adjacent edges at nodes whose degree > Δ*/
        delete_edge( ); /*remove from graph G the edge of longer length that forms the minimum angle*/
        Degree_of_EndNode(edge)--; /*degree of both two end nodes of the edge decrease by 1 */
```

```
        max_deg = find_max_deg( );
    }/* end while*/

/*Step 3: edge_adding */
no_node = find_node( ); /* find all nodes with degree less than degree constraint, no_node is the number of these nodes */
while(no_node >= 2) {
        find_edge( ); /* find a missing edge formed among these nodes that has the shortest length */
        add_edge( ); /* add the edge to the graph */
        Degree_of_EndNode(edge)++; /*degree of both two end nodes of the edge increment by 1 */
         no_node = find_node( );
        } /* end of while */
}
```

Using the proposed NTD algorithm, for the same set of nodes used previously, the constructed Delaunay Triangulation formed at the first step is shown in Figure 3.9. After edge-deleting and edge-adding operations, the final topology is shown in Figure 3.10.

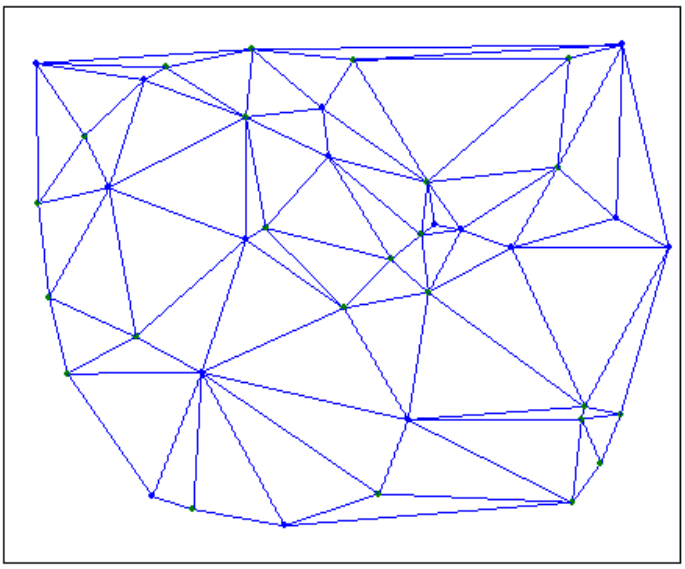

Figure 3.9 Delaunay Triangulation

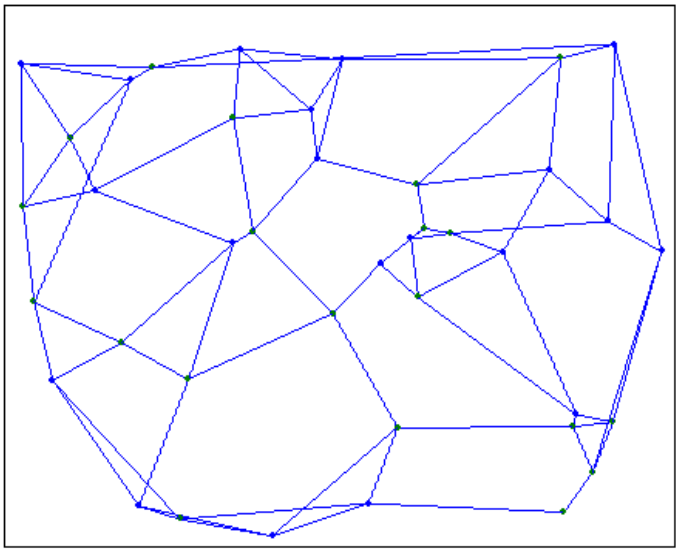

Figure 3.10 Network topology constructed with NTD

Compared with Figure 3.8 constructed with the CN algorithm, FSO links appear to be more divergent in different directions and more evenly distributed with the proposed NTD algorithm.

Here, another example is presented to show the difference between the physical topology constructed with the CN algorithm and the physical topology constructed with the proposed NTD algorithm for a given set of points (or nodes). First, a set of 70 randomly distributed points (or nodes) is generated, as shown in Figure 3.11. Then two different physical topologies of degree 6, constructed with the CN algorithm and the NTD algorithm, are shown in Figure 3.13 and Figure 3.15, respectively.

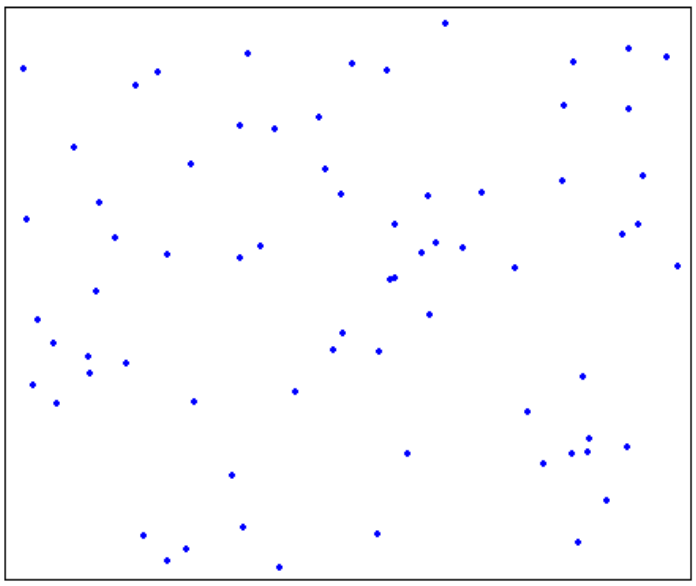

Figure 3.11 70 randomly distributed point-set

Using the CN algorithm, first form a degree-constraint minimum spanning tree shown in the following Figure 3.12.

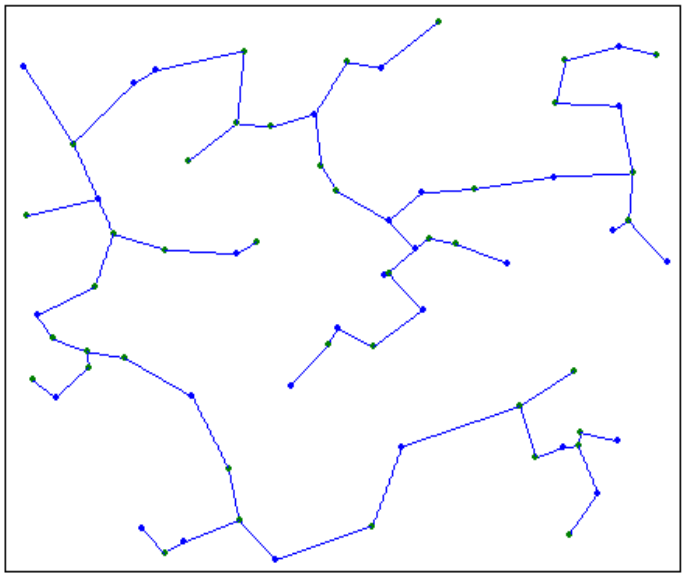

Figure 3.12 A degree-constrained minimum spanning tree

Then as many as possible edges are added under nodal degree-constraint according to [68]. The final constructed graph (or topology) is shown in the following Figure 3.13.

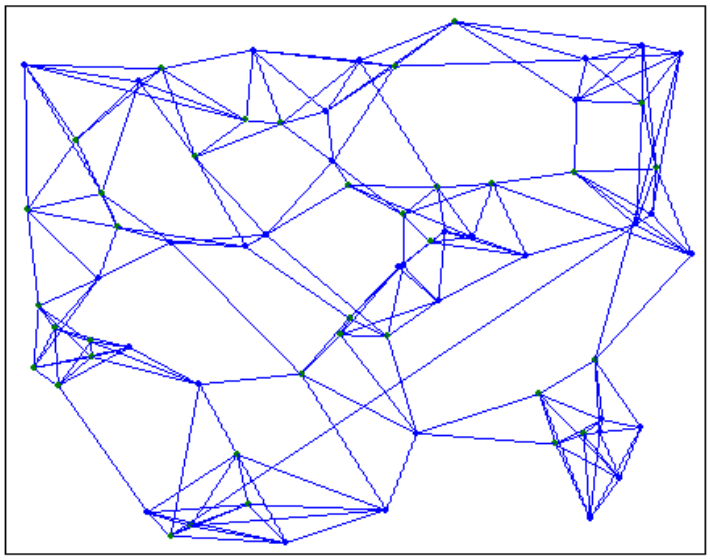

Figure 3.13 The constructed physical topology using CN

Using the proposed NTD algorithm, first form the DT of the given point set. It is shown in the following Figure 3.14.

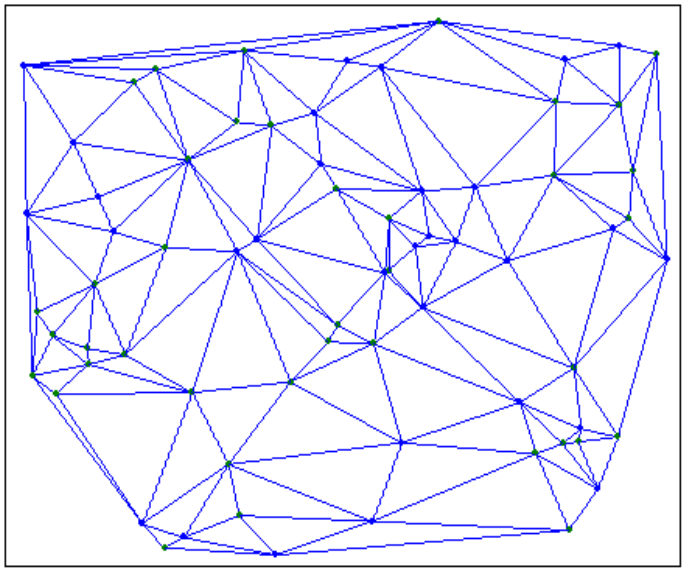

Figure 3.14 Constructed DT graph

Then after edge adding and deleting procedure, the final constructed physical topology is shown in the following Figure 3.15.

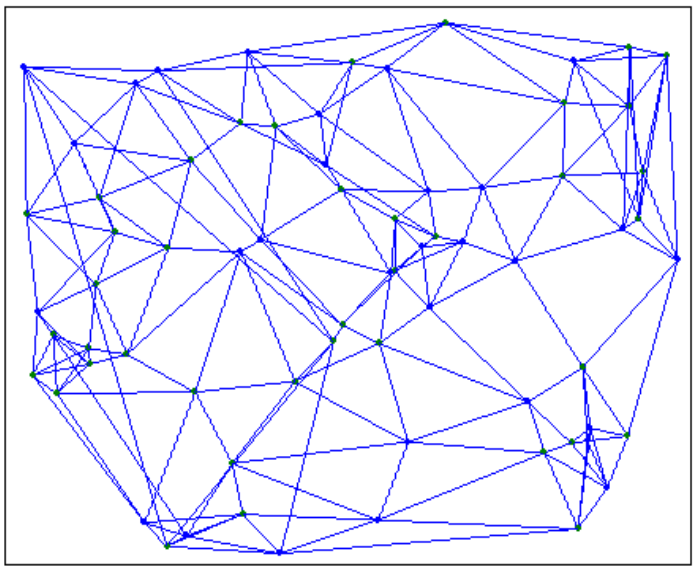

Figure 3.15 Constructed graph using NTD algorithm

Comparing Figure 3.15 with Figure 3.13, it can be easily seen that, links in Figure 3.15 are more evenly distributed. Later in this chapter, it will also be shown through simulations that, the connectivity of the network is not only preserved but also improved for FSO networks constructed with the NTD algorithm.

3.3.3 Advantages of the NTD algorithm

FSO links suffer from a high probability of failure caused by various atmospheric effects and changes in the environment. To deal with FSO link failure, one approach is to increase spatial diversity. Spatial diversity can be achieved through multiple aperture transceiver design [8] to avoid complete

blockage, compensate scintillation, and increase redundancy. However, the multiple aperture design adds complexity to the light being coupled onto receivers effectively. It also adds difficulty for the alignments of multiple transmit and/or receive apertures and maintaining the alignment. At last, the multiple aperture approach adds more complexity on the design of a tracking system, which leads to high overall cost [8].

In the proposed NTD algorithm, an angle enlargement strategy is used to increase spatial diversity of FSO networks without incurring any additional cost. The following shows the advantages of the NTD algorithm in different circumstances.

Under adverse weather conditions such as heavy fog, laser beams (or FSO links) suffer significant attenuation when they go through fog, because the fog aerosols have a comparable size as the wavelengths of the lasers. FSO links may fail because of various atmospheric effects. Generally speaking, most atmospheric effects are highly localized. In the proposed method, we enlarge the angle between adjacent links at an FSO node so that the adjacent links formed at that node travel in diverging directions. In this way, when one link fails, the potential of the failure of the adjacent link is greatly reduced. Figure 3.16 shows the case.

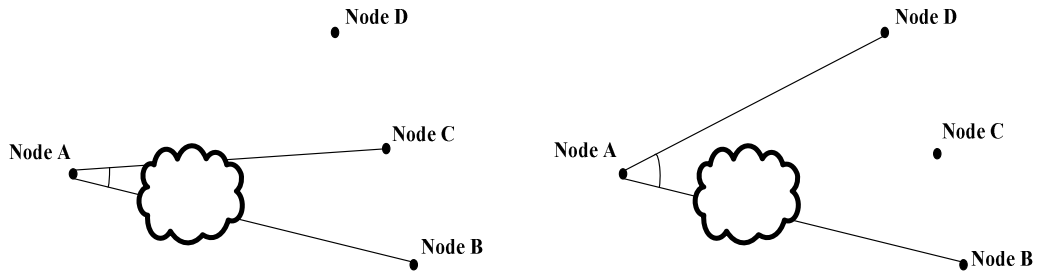

Figure 3.16 Advantage of angle enlargement in case of a temporary blockage

In a similar way, when the laser beam is temporarily blocked by obstructions such as a passing cloud, or flying birds, since the adjacent link points to a much different direction, the chance of the blockage of both links is also reduced. Since a highly sensitive receiver in combination with a large-aperture lens is used in each transceiver for FSO signal reception, natural background light can potentially interfere with FSO signal reception. When the background radiation is associated with intense sunlight, it is called solar interference. Sometimes a FSO link fails for periods of several minutes when the sun is within the receiver's field of view (FOV). Since the angle between adjacent links at an FSO node is enlarged in the proposed NTD scheme, when one FSO link fails because of solar interference, the likelihood that the redundant adjacent link suffers from solar interference is greatly lowered. In fact, a 10^{o} enlargement of the angle at 70^{o} between two adjacent links could make about 3dB decrease of solar power that falls on the redundant receiver surface.

The effect of atmospheric scintillation (or heat shimmer) is very important when FSO links are formed over longer distances. Atmospheric scintillation is defined as the changing of light intensities in time and space at the plane of a receiver that is detecting a signal from a transmitter located at a distance. During midday when the temperature is highest, link failure happens when atmospheric scintillation causes rapid fluctuations of received power. Through enlarging the angle between adjacent links at an FSO node, the two adjacent receivers at that node face much different directions; therefore the probability of both links suffering from atmospheric scintillation during the same period of time is greatly reduced.

To evaluate the performance of constructed FSO mesh networks, four main measures of performance are defined in the following section.

3.3.4 Measures of Performance

The performance of FSO mesh networks is evaluated using four parameters: connectivity, average minimum angle, average minimum hop count, and average link length.

A. *Connectivity*

It is known that the reliability of an FSO mesh network is very important for the overall performance of the network. According to [49], network reliability is

defined as the probability of working nodes connected with functioning links. There are three main measures of network reliability: connectivity, resilience, and performability measures. According to [80], for the majority of the research on network reliability, connectivity is the common measure of network reliability. In this section, connectivity is also used as the measure of network reliability.

Connectivity is defined as the minimum number of nodes that must be removed to disconnect a network. Another measure of interest is link (or edge) connectivity, which is defined as the minimum number of links (or edges) that must be removed to disconnect a network. Link connectivity is extremely important for FSO networks with high probability of link failure. However, it is discussed in [70] that "these definitions address only the worst case concerning the most unfavorable combination of node or edge failures in a network. Alternative and perhaps better metrics for reliability are the averages, over all pairs of nodes, of the minimum number of nodes or edges required to be removed to disconnect them."

Menger's Theorem: *The minimal number of edges separating the source from the destination is equal to the maximal number of edge-disjoint source-destination paths. The minimal number of nodes separating the source from*

the destination is equal to the maximum number of node-disjoint source-destination paths.

According to Menger's theorem [81], between any pair of nodes, two types of connectivity are defined: link connectivity and node connectivity. Link connectivity between any pair of nodes is defined as the maximum number of link-disjoint paths between the pair of nodes, and node connectivity between any pair of nodes is defined as the maximum number of node-disjoint paths between the pair of nodes.

In this section, the minimum link connectivity of an FSO mesh network is defined as the minimum of the maximum number of link-disjoint paths among all pairs of nodes, and the minimum node connectivity as the minimum of the maximum number of node-disjoint paths among all pairs of nodes in the network. They are worst-case measures of network reliability. This section also defines average link connectivity as the average of the maximum number of edge-disjoint paths among all pairs of nodes, and average node connectivity as the average of the maximum number of node-disjoint paths among all pairs of nodes. They are the average-case measures of network reliability.

It can be easily shown that both the link connectivity k' and the node connectivity k between a pair of nodes are equal to or less than the pairwise

degree δ of the nodes, where the pairwise degree is the smaller degree of the pair of nodes being considered. The pairwise degree is thus the upper bound of link and node connectivity. The minimum pairwise degree is the upper bound of both the minimum link connectivity and the minimum node connectivity of an FSO network. The average pairwise degree is the upper bound of the average link connectivity and average node connectivity of a network. Since node-disjoint paths between any pair of nodes must also be link disjointed, and it's not always true conversely, it is obtained that: $k \leq k' \leq \delta$.

Both link connectivity and node connectivity reflect path diversity of an FSO mesh network. Increased path diversity leads to high reliability of FSO mesh networks.

B. *Average Minimum Angle*

Average minimum angle is defined as the average of the minimum angles between adjacent links at all FSO nodes. For an N node FSO network, the average minimum angle can be expressed as

$$\theta_{avg} = (\sum_{i=1}^{N} \theta_i) / N$$

Where θ_{avg} is the average minimum angle, θ_i is the minimum angle formed at node *i*.

Average minimum angle is used as a parameter to measure the dependency of link failure events of FSO networks in a dynamic environment. The larger the angle between any two adjacent links, the lower the probability of the failure of both links.

C. *Average minimum hop count*

The average minimum hop count is defined as the average of the minimum number of hops among all pairs of nodes in an FSO network. For an N node FSO network, it can be expressed as

$$HC_{avg} = \left(\sum_{s=1}^{N-1}\sum_{t=s+1}^{N} HC_{\min}(s,t)\right) / \left(\frac{N\times(N-1)}{2}\right)$$

Where HC_{avg} denotes the average minimum hop count, $HC_{\min}(s,t)$ denotes the minimum hop count between node s and node t. $\frac{N\times(N-1)}{2}$ is the total number of node pairs in an N node network.

In FSO networks, the propagation delay of light signals can be ignored because of the high speed of light and the fact that link lengths are short; however, the delay per hop can not be neglected. As an example, for OmniNode (an FSO node), the average delay per hop is about 0.1ms

excluding queuing delay [82]. The total delay between a pair of nodes (source node and destination node) equals the delay per hop times the minimum hop count between them.

Since the total delay between a pair of nodes is proportional to the minimum hop count between them, the average minimum hop count is used as the measure of average delay performance of FSO networks. The maximum of the minimum hop counts corresponds to the maximum delay. It is used as the worst-case delay performance of FSO networks. A lower average minimum hop count also enhances the reliability of an FSO network.

D. *Average link length*

Average link length is defined as the average length of all FSO links in an FSO network. For an FSO network with L links, it can be expressed as

$$Length_{avg} = (\sum_{i=1}^{L} Length_i) / L$$

Where $Length_{avg}$ is the average link length. $Length_i$ is the length of link i. L is the total number of links in the network.

Because of atmospheric attenuation, shorter FSO links have higher system margins. Thus, the shorter the average link length, the higher the average system margin, and therefore better performance of FSO links can be achieved.

Simulations have been done to evaluate the performance of FSO mesh networks constructed with different topology design algorithms. In the next section, the simulation results are shown and analyzed.

3.3.5 Simulation results and analysis

Performance measures defined in the last section are calculated based on topologies constructed with the CN algorithm and the NTD algorithm. The results for each are compared.

A. *Connectivity*

(1). Deterministic Connectivity

To compare the NTD algorithm with the CN algorithm, 50 Poisson-distributed point sets each with 40 nodes are generated with random seeds from 1 to 50. All 40 nodes are located in a 40×40 square. Each node has 4 transceivers that can be used to build links with other nodes.

The connectivity of a static FSO network is evaluated. The minimum connectivity and the average connectivity are calculated. There are 40*(40-1)/2 = 780 possible pairs of nodes in a 40-node topology.

Table 3.1 Comparison of connectivity between CN and NTD

	CN	NTD
mini. δ	3.88	3.52
mini. k'	2.28	3.36
mini. k	1.46	2.0
avg. δ	3.99	3.986
avg. k'	3.548	3.96
avg. k	2.7	3.51

Table 3.1 shows the results averaged over 50 different topologies. mini. is short for minimum. avg. is short for average. δ denotes pairwise degree. k' denotes link connectivity. k denotes node connectivity.

The simulation results show that even though NTD forms smaller minimum pairwise degree, it outperforms the CN model by 47.4% on the minimum link connectivity, and 37% on the minimum node connectivity. Similarly, the NTD has smaller average pairwise degree; however, it outperforms the CN by 11.6% on the average link connectivity, and 30% on the average node

connectivity. The increase of link connectivity and node connectivity for NTD over CN comes mainly from a more even distribution of FSO links.

Since the minimum pairwise degree and average pairwise degree are the upper bounds of minimum connectivity and average connectivity, it is observed that the connectivity of a topology constructed with NTD is very close to the maximum connectivity.

(2). Link Connectivity under Failures

Since link failure usually happens in a dynamic environment for FSO networks, it should be taken into consideration in the network reliability measure. Link connectivity under failures reflects the robustness of FSO networks in a dynamic environment. In the simulation, the Monte Carlo model is employed to simulate the dynamic feature of FSO networks. Link failures are treated as random events and independent events from each other.

To do the simulation, 70 randomly distributed nodes are generated in a 70×70 square with each node having degree constraint 5.

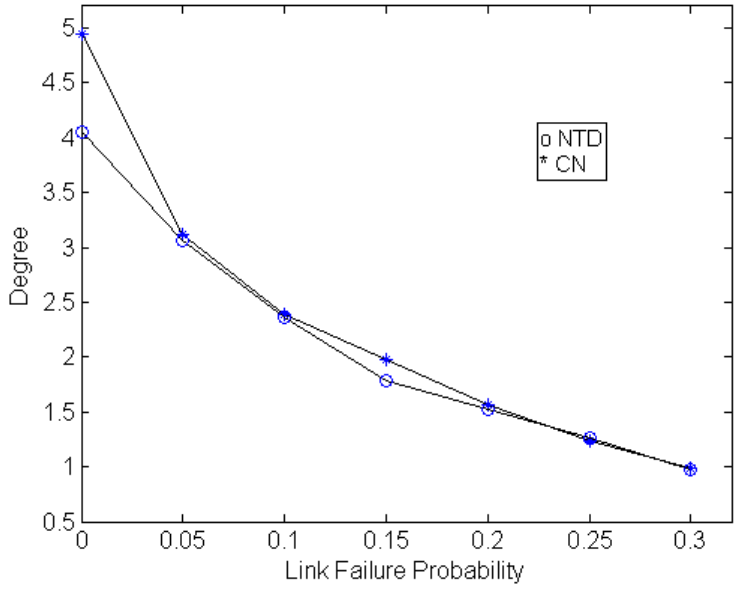

Figure 3.17 Minimum pairwise degree under link failure

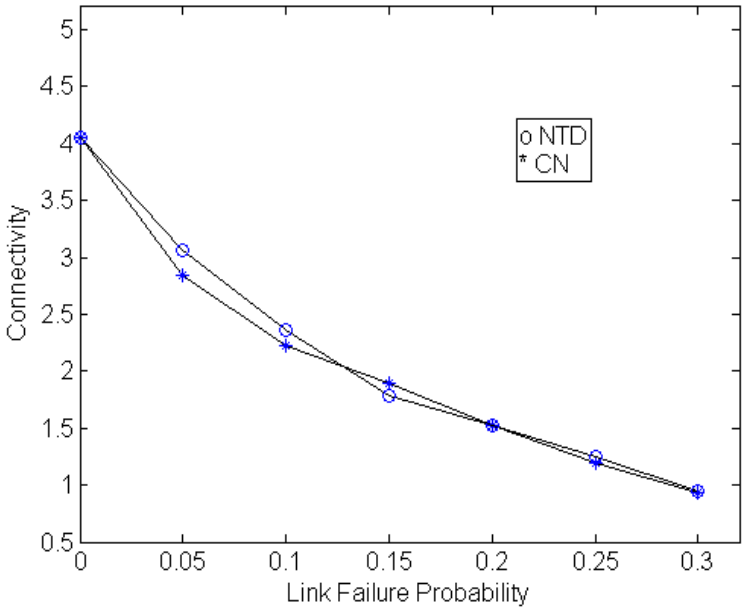

Figure 3.18 Minimum link connectivity under link failure

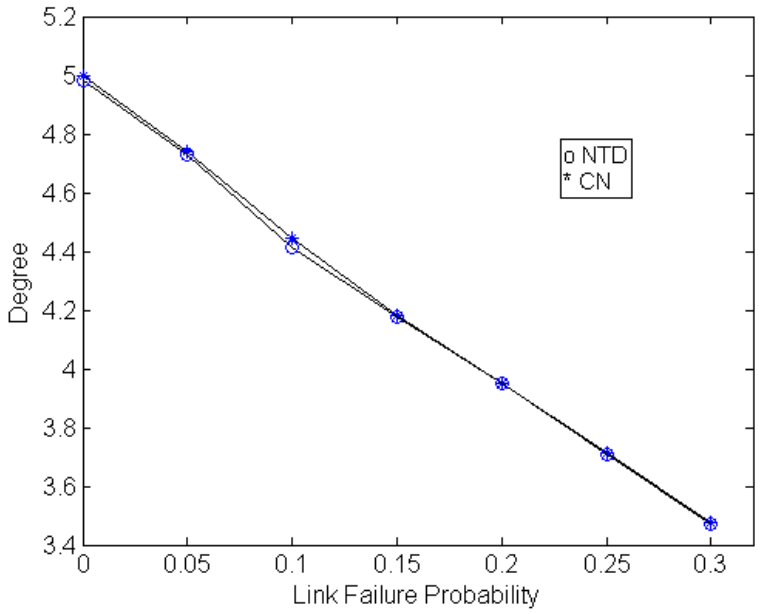

Figure 3.19 Average pairwise degree under link failure

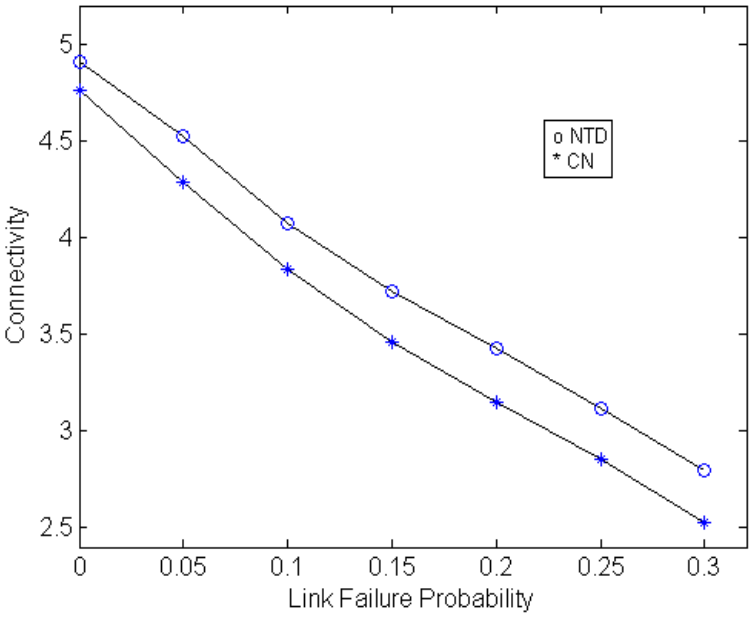

Figure 3.20 Average link connectivity under link failure

Figure 3.17 to 3.20 show the simulation results averaged over five different topologies. Both the minimum link connectivity and the average link connectivity are plotted against link failure probabilities from 0.0 to 0.3. Figure 3.18 and 3.20 show the minimum link connectivity and average link connectivity against link failure probabilities, respectively. Minimum pairwise degree and average pairwise degree are plotted against link failure probabilities in Figure 3.17 and 3.19, respectively. One can observe clearly that even though the resulting minimum pairwise degree and average pairwise degree are a bit smaller for NTD over CN, the minimum link connectivity and the average link connectivity against link failure probabilities are higher for NTD over CN in most cases.

B. *Average Minimum Angle*

To calculate the average minimum angle for different topologies, the simulation was performed with 40 Poisson-distributed FSO nodes located in a 40×40 square. Each FSO node has 4 transceivers. 20 different topologies are generated with random seeds from 1 to 20. Simulation results are averaged over these 20 different topologies.

Table 3.2 Average minimum angle comparison between CN and NTD

	CN	NTD
Avg. min. angle	23.35	33.57

Simulation results show that the average minimum angle at any node of the topology constructed with the CN algorithm is 23.35^{o}, whereas the average minimum angle is 33.57^{o} with the NTD algorithm. There is a 43.77% increase of average minimum angle for NTD over CN.

C. *Average Minimum Hop Count*

To compare the NTD algorithm with the CN algorithm, the same 20 sets of nodes as those used previously are also used here. Based on them, 20 different topologies constructed with CN and NTD are formed, respectively, for the measurement of minimum hop count.

Table 3.3 Hop count comparison between CN and NTD

	CN	NTD
Max. hopc.	7.9	6.8
Avg. hopc.	3.8633	3.42045

Table 3.3 shows the simulation results averaged over 20 different topologies. There is a 16.17% decrease of maximum minimum hop count for NTD over CN, and a 12.9% decrease of average minimum hop count for NTD over CN.

D. *Average Link length*

The same 20 different topologies are used for the measurement of average link length.

Table 3.4 Average link length comparison between CN and NTD

	CN	NTD
Avg. link length	6.79	7.35

The above simulation results show that the average link length of the topology constructed with the CN algorithm is 6.79; the average link length is 7.35 with the NTD algorithm. There is only 7.6% decrease of average link length for CN over NTD.

3.4 Summary

In this chapter, a topology design problem for FSO mesh networks is stated. Previous research is reviewed. A network topology design (NTD) algorithm is proposed for the physical layer configuration of FSO mesh networks. An initial configuration is created by using Delaunay Triangulation which maximizes the minimum angle of the mesh topology. The proposed algorithm then creates higher path diversity by deleting and adding edges in the configuration such that the degree constraint of the network is met while at the same time minimum angles at all applicable nodes are enlarged. Improvement in the performance of FSO networks designed using the proposed NTD algorithm is verified through extensive simulations. Compared to the CN algorithm, the proposed NTD algorithm results in higher link connectivity and node connectivity, larger average minimum angle, and lower minimum hop count.

Chapter 4

The NTD Algorithm in 3-dimensional Space

Abstract: This chapter discusses errors caused in the NTD algorithm proposed in Chapter 3 because of the 2 dimensional (2-D) approximations of 3 dimensional (3-D) FSO node locations. A 3-D NTD algorithm is therefore proposed and analyzed that can not only avoid all the errors, but also achieve high spatial diversity and low average link length.

4.1 Introduction

One of the major advantages of FSO networks is the ease with each FSO network can be deployed in any environment, including when the terrain is difficult and the heights of all FSO nodes are not identical. An equally compelling case is for downtown FSO deployment where the heights of all the buildings are not identical. The topology design algorithm presented in Chapter 3 is based on 2-D Delaunay Triangulation where the given set of points in 3-D space is treated as lying in the plane z=0. Obviously, if the heights of the FSO nodes are not identical, this condition does not hold.

This chapter develops a means by which the physical topology design problem in a 3-D environment can be effectively addressed.

4.2 Review of the properties of an optimal physical topology for FSO mesh networks

Based on the analysis made in Chapter 3, an optimal physical topology of an FSO mesh network should have the following properties.

- FSO links at any node should have high angular divergence, which implies high spatial diversity, in order to make the thus formed FSO network more tolerant in a dynamically changing environment.
- It should be difficult to disconnect an FSO network by removing a few links or nodes, which implies high redundancy.
- Although all links are assumed to be within the allowable transmission range, shorter FSO links have higher system margin; therefore in the topology design of FSO networks, nearer nodes should have a higher priority of being connected to a given node.

4.3 Errors caused by the 2D-approximation of a 3D terrain

The previously proposed NTD algorithm is reviewed first. Given the location information of all FSO nodes, based on the assumptions made in Chapter 3, the NTD algorithm operates as follows.

Step 1: Construct the DT of the given set of nodes.

Step 2: For nodes with degree higher than Δ in the DT, remove the longer edge of two adjacent edges that form the minimum angle. Repeat until the degree constraint of each node is met.

Step 3: For nodes with degree less than Δ, edges are added in ascending order of their lengths without violating the degree constraint at any node.

Taking a 2-D projection of a 3D-based location as in step 1, 2, and 3 will result in the following errors.

First, Step 1 starts with building a 2-D DT graph that has not only high redundancy, but also high spatial diversity. The DT is constructed by operating on a set of points lying in the 2-D plane, z=0. Even though the 2-D DT maximizes the minimum angle of all triangles in the 2-D plane, the minimum angle in a 2-D plane is not necessarily to be the same as in the corresponding 3-D graph of triangulation. Therefore, it results in error when applied to 3-D space. We prove this by a counterexample which follows.

The coordinates of four points considered in the X, Y, Z co-ordinates are as follows:

A = 0, 0, 0

B = 1.5, 0, 0

C = 1, 2, 0

D = 0, 1.5, 2

The four points, under consideration, A, B, C, and D are shown in Figure 4.1. Points A, B, and C lie on the X-Y plane while D does not. D' is the projection of D on the X-Y plane.

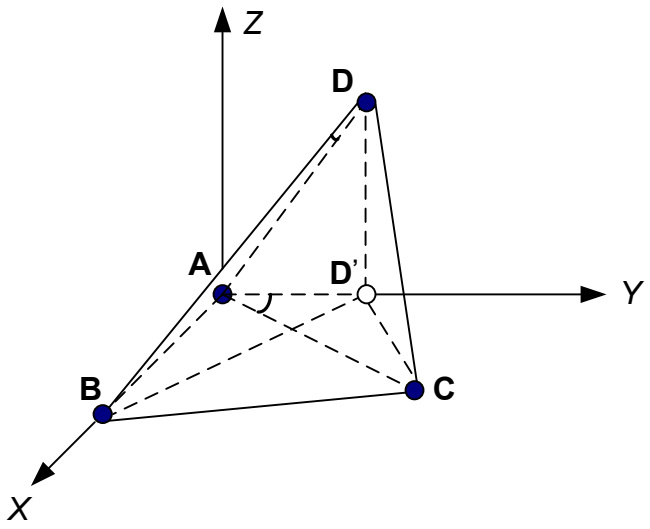

Figure 4.1 Comparison between 2D minimum angle and 3D minimum angle

After geometric computations, the following results are obtained. The minimum angle $\angle CAD'$ in the 2-D plane (containing points A, B, C, and D') is equal to 26.57^{o}. The minimum angle in the 3-D space (containing points A, B, C, and D) is $\angle ADB$, which is equal to 30.96^{o}. Since the minimum angles in the 2-D and 3-D configurations are different, the maximization of the minimum angle will

have to adopt a different process. In this particular case, in the 2-D plane, the shared edge of two adjacent triangles has to be BD in order to maximize the 2-D minimum angle; whereas in 3-D space, the shared edge has to be AC in order to maximize the 3-D minimum angle. This angle maximization is still done using edge flipping technique. Figure 4.1 illustrates the case. It can be observed that the likelihood of this situation arising will increase as the difference between the heights of the nodes increases.

Step 2 deletes edges in order to satisfy the nodal degree constraint, as well as further increasing spatial diversity among FSO links at all applicable nodes. Step 2 also may cause error when the minimum angle found is not minimal in 3-D space. Figure 4.2 shows the case.

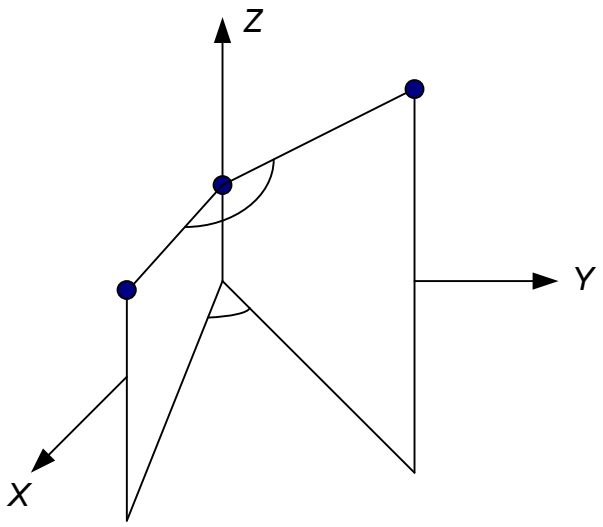

Figure 4.2 Relationship between a 3-D angle and its corresponding 2-D angle

Step 3 adds edges to the graph in the ascending order of their length. The length of each edge is actually calculated based only on their 2-D coordinates; therefore Step 3 may also cause error when the length of an edge in the 3-D space is not the same as the length of its projection on the 2-D plane. Based on the above analysis, the proposed NTD algorithm is not optimal when the heights of FSO nodes are not identical in a 3-D terrain.

To avoid the errors caused in the 2-D NTD algorithm, the algorithm needs to be extended to operate on a given node set in the 3-D space. In the proposed heuristic approach, the 3-D graph of triangulation, formed by mapping a 2-D planar graph of triangulation to the 3-D node set, is used as a starting point, instead of starting with a 3-D DT. There are two reasons for that.

- The computational complexity of a 3-D DT is considerably higher than a 2-D DT. For a point set of n points, the worst-case time complexity for a 2-D DT is O(n log n) [83], whereas for a 3-D DT it is $O(n^2)$ [84].
- In a 3-D DT of a point set of n points, the number of tetrahedra is $O(n^2)$ [83], thus leading to a much higher storage requirement.

4.4 The 3D NTD algorithm

Based on the above constraints, a heuristic 3-D NTD algorithm is stated as follows.

Step 1: Construct a planar graph of triangulation of a given set of nodes in 3-D space lying in the 2-D plane (z=0).

Step 2: Map the connectivity information of the 2-D graph on to the given 3-D node set, forming a 3-D graph of triangulation.

Step 3: For any two adjacent triangles of the 3-D graph of triangulation, flip their shared edge, based on the evaluation of all the angles formed, in order to maximize the minimum angle.

Step 4: Among nodes with degree higher than degree constraint in the 3-D topology, find the node with the minimum angle formed by its two adjacent links; remove the longer edge of two adjacent edges that form the minimum angle at that node. Repeat until the degree constraint of each node is met.

Step 5: In 3-D space, for nodes with degree less than degree constraint, add edges in the ascending order of their lengths without violating the degree constraint at any node.

It can be observed that the proposed 3-D algorithm will result in a physical topology with larger minimum angles and shorter average link lengths compared to the case if the 2-D NTD algorithm were executed on a planar projection of the 3-D node set, and the resulting topology simply extended in the 3-D space. The larger minimum angle results from the fact that the

extended 3-D NTD algorithm deletes edges based on the actual 3-D minimum angle. During edge adding procedure, the 3-D NTD adds edges in the ascending order of their actual 3-D edge length; therefore, the 3-D NTD results in shorter average link length. We conclude that the 3-D NTD algorithm effectively results in a configuration that is well suited to the actual 3-D space. The 3-D NTD algorithm is expected to achieve higher spatial diversity as well as shorter average link length when applied to a 3-D terrain.

Chapter 5

Routing in FSO Mesh Networks

Abstract: This chapter addresses the routing problem in degree-constrained FSO mesh networks. In this chapter, four different routing algorithms are proposed. Their performances are evaluated through simulations for a number of FSO mesh networks with different topologies and nodal degrees. The performance parameter against which these algorithms are evaluated is the mean end-to-end delay. The proposed Least Cost Path (LCP) routing algorithm, which is based on minimizing the end-to-end delay, is considered as the bench mark. The performances of each of the three other proposed algorithms are evaluated against the bench mark. The proposed Minimum Hop Count with Load Balancing (MHLB) routing algorithm is based on the number of hops between the source and the destination node to route the traffic. Simulation shows that the MHLB routing algorithm performs best in most cases compared to the other two. It results in minimum average delay and least blocked traffic.

5.1 Introduction

Network topology and routing are the two critical factors that affect the performance of FSO networks. Traditionally, for wired communication networks such as fiber-optic networks, a fixed physical layer topology is formed based on external traffic flow requirements, and performance considerations. Routing is the task of finding optimal logical connections that can be mapped on to the physical layer topology in order to achieve low delay, high throughput, or reduced congestion.

5.1.1 Previous works

Research in [85] presents a delay-constrained minimum hop (DCMH) distributed routing algorithm for real time communication applications. An optimal diverse routing algorithm is proposed in [86] to find the shortest pair of physically-disjoint paths in order to improve the reliability of fiber optical networks. Reference [87] presents an algorithm that computes the shortest path from a given source to a destination for any number of hops for QoS routing. Research in [88] extends the work in [87], and proposes an All Hops Shortest Paths (AHSP) algorithm to compute the shortest path with hop count limitation in order to find a feasible path. An algorithm is proposed in [89] to measure the average delay of a packet in packet switched networks under conditions of random failure and specific priority routing discipline. For multi-path packet switching communication networks, traffic splitting is necessary to

spread traffic along multiple paths. However none of the above mentioned investigations considers splitting the traffic so that desired performance benchmarks might be realized.

To achieve an equitable traffic load distribution, reference [90] proposes a framework for packet-based load sharing in multi-path communication networks. The same authors also propose in [91] a framework for flow-based traffic splitting in multi-path communication networks. Although their proposed schemes result in low mean squared workload deviation, the end-to-end path delay is not considered in their work. Reference [92] proposes an algorithm to distribute packets to a set of active paths in a round robin fashion. A load-balanced routing scheme is proposed in [93] to randomly distribute the traffic load over all available paths to the destination for real time applications. However with different multiple paths, using the proposed algorithms in [92, 93] to spread traffic along those paths may not lead to the minimized end-to-end path delay. A survey is presented in [94] that introduces several approaches to solve multi-constrained paths problem for QoS routing.

All of the above mentioned routing approaches assume a given physical layer topology. However, for FSO networks, current approaches [67], [95] have combined both topology design and routing problems into one making use of

the auto-tracking function of FSO nodes. In these approaches, logical topologies are first calculated at upper layer. Physical layer topologies are then gradually formed based on the calculated logical topologies. Since the mapping of physical layer topology to logical topology involves a number of rounds of mechanical movements of transceivers in FSO nodes, and each movement of a transceiver takes about 500ms for alignment purpose only [67]; these approaches are, in general, not practical for FSO communication networks.

5.1.2 The proposed framework for routing

In this chapter, the routing problem is addressed using an approach that is similar to the wired networks. In Chapter 3, a topology design algorithm has been presented to construct a highly reliable physical layer topology for an FSO mesh network [96]. Now, based on a given physical layer topology, and external traffic demands, the objective here is finding an optimal logical topology that can be mapped on to the physical layer topology in order to achieve low average packet delay. Four different routing algorithms, including the benchmark routing algorithm, are proposed in this chapter. Through extensive simulations, it is shown that the proposed minimum hop count with load balancing (MHLB) routing algorithm leads to the best overall performance. The MHLB routing algorithm has computational simplicity while at the same

time matching the performance level achieved by the benchmark routing algorithm.

This chapter is arranged as follows. Section 5.2 presents the problem that needs to be solved. A queuing system model is introduced in Section 5.3. Section 5.4 presents the mathematical background. The four proposed routing algorithms are presented in Section 5.5. Section 5.6 shows the simulation results. Section 5.7 concludes this chapter.

5.2 Problem statement

Three factors can affect the delay performance of FSO networks: physical layer topology, external traffic demands, and routing strategy. It is assumed that the physical layer topology and external traffic demands are given. To simplify the problem, all link capacities are assumed to be the same. This is generally the case for FSO networks. The problem addressed in this chapter can be stated as follows: find an optimal routing strategy that minimizes the average end-to-end delay T. It can be easily observed that the routing problem is a flow assignment (FA) problem [97]. The FA problem can be stated as follows.

Given: network topology and external traffic flows

Minimize: T

With respect to: $\{\lambda_i\}$, i =1, 2, …, L

λ_i is the traffic load on link i. The lambdas are determined by the specific routing strategy deployed.

5.3 System model

In this chapter, a communication network is modeled as a network of queues. It is analyzed based on Jackson's theorem. The theorem is based on three assumptions [48]: First, each node in the queuing network provides an independent exponential service. Second, external traffic arrives at any node with a Poisson rate. Third, traffic departs from a node with a fixed probability. To illustrate a queuing network, given the physical layer topology of a five-node network shown in Figure 5.1, the network can be modeled as a network of queues shown in Figure 5.2.

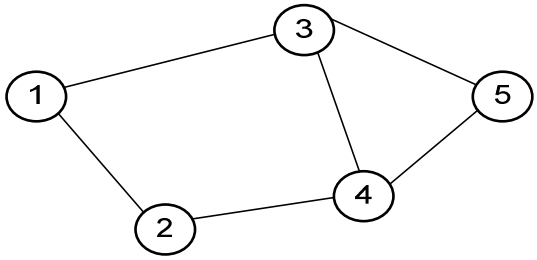

Figure 5.1 A five-node network

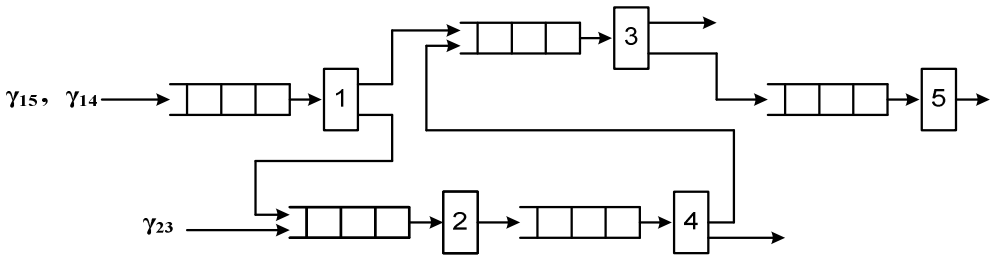

Figure 5.2 A network of queues

According to Jackson's theorem, each node may be analyzed separately from others as an independent M/M/1 or M/M/N model [48]. It is assumed that the traffic arrival rate is Poisson, and the service time distribution is negative exponential. For a Poisson arrival process, the following equation applies.

$$P_n(t) = \frac{(\lambda t)^n}{n!} e^{-\lambda t}$$

Where:

- t is used to define the interval 0 to t
- n is the total number of arrivals in the interval 0 to t.
- lambda is the total average arrival rate in arrivals/sec.

By substituting n with 0, the following equation is obtained:

$$P_0(t) = e^{-\lambda t}$$

It shows that the probability that no arrival takes place during an interval from 0 to t is negative exponentially related to the length of the interval. Similarly, the service times for customers are also negative exponentially distributed (i.e. generated by a Poisson process).

For packet switching networks, it looks like that this approach of treating each node as an independent M/M/1 or M/M/N model has a flaw. The reason is that

since the length of a packet is the same at each transmission link, and the arrival process to each queue is correlated to the service process, the service time distribution is not independent. However, it is discussed in [98] that, for external traffic entering the network, this assumption is quite accurate. The reason is that the collective interarrival times and lengths of messages generated by the entire population of subscribers exhibit an independence, since the length of a message generated by any particular subscriber is completely independent of the arrival times generated by the other subscribers. It is similar to the internal traffic of packet switching networks. In general, there is more than one channel delivering messages into any particular node (in addition to those messages arriving from the external source feeding this node), and more than one channel transmitting messages out of this node. Because of this effect of entry and exit of traffic, it has been demonstrated in [98] that the arrival process at each node can be approximated by the Poisson process.

5.4 Mathematical background:

A degree-constrained FSO mesh network is treated as a graph G(N,L) with N representing the set of nodes and L representing the set of links. The following notations are used.

A=[γ_{jk}] denotes the N x N traffic matrix, where

γ_{jk} : external traffic flow entering node *j,* and destined to node *k*

B=[ρ_{st}] denotes the N x N link utilization matrix, where

ρ_{st} : utilization of link between node *s* and node *t*.

μ : departure rate of any link

λ_i : traffic load on link *i*

λ: total internal traffic load

γ: total external traffic demand

T: average delay for all packets traveling through the network

Assume that the external traffic flow requirement from a source node j to a destination node k is γ_{jk}, then the total external traffic flow γ (in packets per second) that is offered to the network can be expressed as

$$\gamma = \sum_{j=1}^{N} \sum_{k=1}^{N} \gamma_{jk} \qquad (1)$$

Since a packet may travel multiple hops from the source to the destination, the total internal traffic flow λ in the network will be higher than the external offered traffic. The total internal traffic load in the network is therefore given as

$$\lambda = \sum_{i=1}^{L} \lambda_i \qquad (2)$$

It can be seen that the total internal traffic flow depends on not only the external offered traffic, but also the actual paths taken by packets through the network. The total traffic load on each individual link is determined by both the offered traffic flows, and the routing algorithm.

Since each FSO link is actually a directional light beam, an FSO light signal propagates at light speed. With limited FSO link length (up to 4 km), the propagation delay can be neglected; therefore when a packet travels along its multi-hop path, it is served at a node, and then considered to go directly to the next node on its path. According to Little's formula, for link i in the network, the average number of packets r_i waiting and being served for that link is given by

$$r_i = \lambda_i T_{ri} \qquad i = 1, 2, \ldots, L$$

Where T_{ri} denotes the average residence time for packets waiting and being served for that link. Then the average total number of packets resident in the

whole network is given by $\sum_{i=1}^{L} \lambda_i \ T_{ri}$. Since the total number of packets in the network can also be expressed as γ T; the average delay T is given by

$$T = \frac{1}{\gamma} \sum_{i=1}^{L} \lambda_i \ T_{ri} \qquad (3)$$

By applying the M/M/1 model,

$$T = \frac{1}{\gamma} \sum_{i=1}^{L} \frac{\lambda_i}{\mu - \lambda_i} = \frac{1}{\gamma} \sum_{i=1}^{L} \frac{\lambda_i / \mu}{1 - (\lambda_i / \mu)} = \frac{1}{\gamma} \sum_{i=1}^{L} \frac{\rho_i}{1 - \rho_i} \qquad (4)$$

Because of the separatibility [97] of each component at the right hand side of equation (4), the sensitivity of the average delay T to the utilization of link *i* can be expressed as

$$\frac{\partial T}{\partial \rho_i} = \frac{1}{\gamma (1 - \rho_i)^2}, \quad i = 1, 2, \ldots, L \qquad (5)$$

Further,

$$\frac{\partial^2 T}{\partial \rho_i^{\ 2}} = \frac{2}{\gamma (1 - \rho_i)^3}, \quad i = 1, 2, \ldots, L \qquad (6)$$

Since the utilization of link *i*, $\rho_i = \lambda_i / \mu$, always satisfies that $0 \leq \rho_i < 1$ to keep the network in a stable state; therefore, $\frac{\partial^2 T}{\partial \rho_i^2} > 0$ for all *i* under the link utilization constraint. It can be concluded that T is a convex function of link utilization. It shows that with the increase of link utilization ρ_i, the growth of T becomes faster. Therefore, an optimal routing strategy should keep link utilization of each link minimal in order to minimize the average delay T. The total internal traffic flow in the network also affects the average delay T; therefore, given external traffic flow requirements and physical layer topology of a network, an optimal routing algorithm should be able to minimize the total internal traffic flow of the network in order to minimize the average delay T.

Based on above analysis, the properties of an optimal routing algorithm are specified as:

- For all links in the network, the link utilization constraint has to be satisfied, i.e., $0 \leq \rho_i < 1$, $i = 1, 2, \ldots, L$.
- The link utilization of each link has to be kept as low as possible, which means that links with low utilization should have higher priority of being chosen to route a given traffic flow demand.

- Given physical layer topology and external traffic flow requirements, the total internal traffic should be kept as low as possible through routing in order to decrease the average delay.

5.5 Proposed routing algorithms

The traffic matrix is constructed first. Each entry of the traffic matrix consists of source node j, destination node k, and required traffic flow γ_{jk}, where j = 1, 2, … , N, k = 1, 2, … , N. If $j = k$, then γ_{jk}=0. The link utilization matrix is constructed as follows. Each entry of the link utilization matrix consists of node s, node t, and link utilization ρ_{st}, where s = 1, 2, … , N, t = 1, 2, … , N. If there is no direct link between node s and node t, or $s = t$, then set ρ_{st} = 1. Otherwise, it sets to 0. For practical reasons and for simplification, the maximum link utilization $\rho_{\max}$ of each link is set as 0.8 (to keep delay within bounds). Because of this link utilization constraint, all traffic that can not be routed is regarded as blocked traffic. Four different routing algorithms are proposed as follows.

5.5.1 Least Cost Path routing algorithm (LCP)

Assume that the existing traffic load on link *i* is λ_i^*, or the existing link utilization of link *i* is $\rho_i^* = \frac{\lambda_i^*}{\mu}$. Using equation (5), we compute the cost (the increment of average delay) of routing traffic flow γ_{jk} through link *i* as

$$Cost(i) = \left.\frac{\partial T}{\partial \rho_i}\right|_{\rho_i = \rho_i^*} \times \frac{\gamma_{jk}}{\mu} = \frac{1}{\gamma(1-\rho_i^*)^2} \times \frac{\gamma_{jk}}{\mu} \qquad (7)$$

Therefore, the total cost of routing traffic γ_{jk} through a path of *m* links is $\sum_{i=1}^{m} Cost(i)$.

In order to minimize the average delay T, each traffic demand is routed through the least cost path. The proposed least cost path routing algorithm is as follows.

1. Set $\rho_{\max}$ =0.8. Route all one hop count traffics under the constraint that $\rho_i \leq \rho_{\max}$. Update traffic matrix and link utilization matrix.
2. Arrange all traffic demands in the decreasing order. If the maximum traffic demand is 0, then stop.
3. Starting from the heaviest traffic demand, find the least cost path to route the traffic under the constraint that $\rho_i < \rho_{\max}$ for any link *i* on the path. Because of the upper bound of link utilization, the part of traffic

that can't be routed through the path remains unrouted. Update traffic matrix and link utilization matrix. If no such path exists, consider next traffic demand. Repeat Step 3 until all traffic demands are considered. Go to Step 2.

In the proposed LCP routing algorithm, Dijkastra's algorithm is used to find the least cost path at step 3 in order to route a given external traffic demand. Link cost is computed according to equation (7). Dijkastra's algorithm has been introduced in Chapter 2.

Given network topology and link cost information, an example is given here on how to find the least cost path to route a given traffic at step 3. For a six nodes network of degree three shown in Figure 5.3, assume all link costs (the delay computed in advance) are as shown in the figure. To route a given traffic from source node A to destination node F, the algorithm proceeds according to the Dijkstra’s algorithm but under the link utilization constraint. It operates as follows.

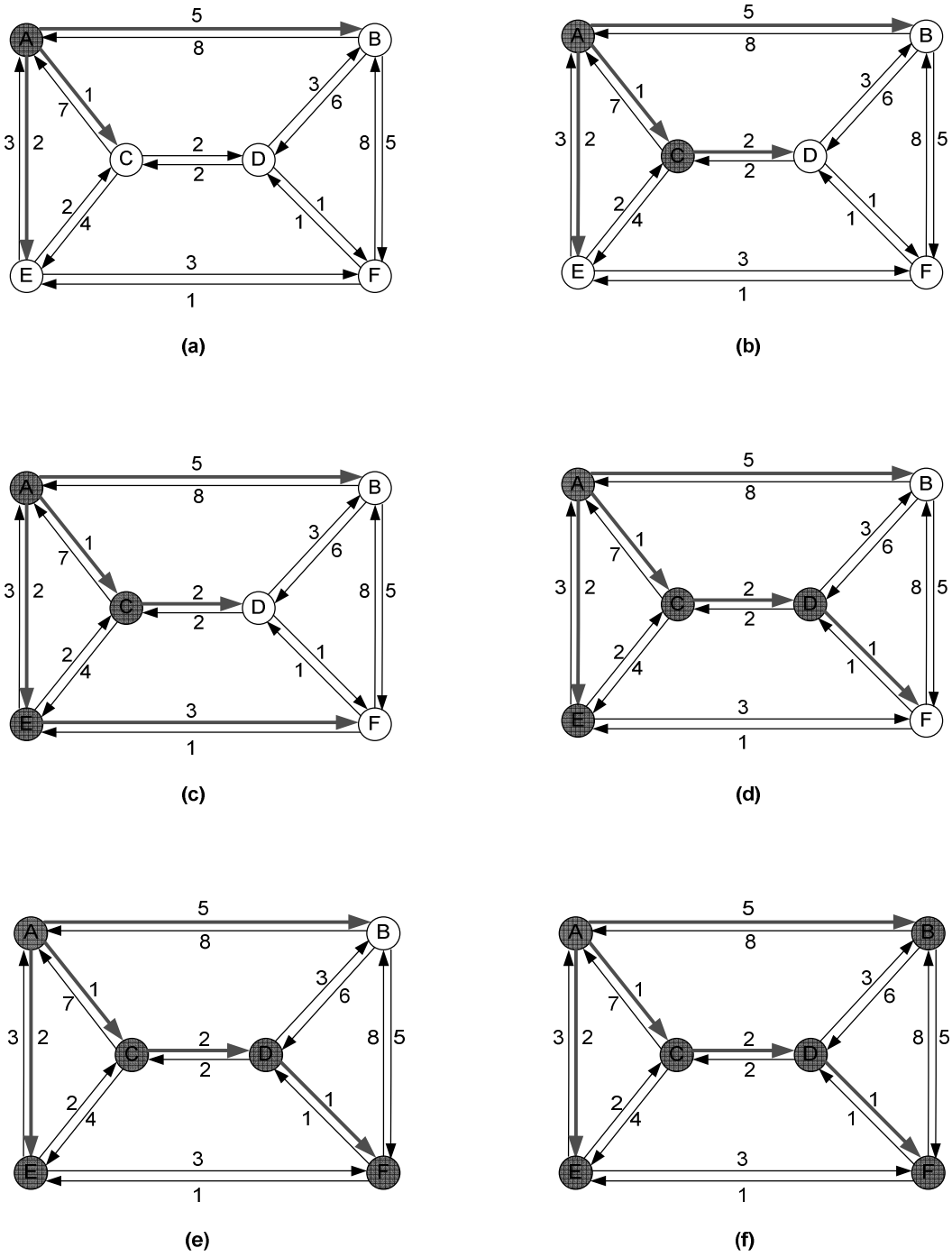

Figure 5.3 Least cost path routing

First the source node A and its edges (AB, AC, AE) are included in a Tree. Then since the path A-C has the least cost, node C and its edge CD is included in the Tree. At the next step, since path A-E has the least cost, node E and its edge EF are included in the Tree. Among path A-B, A-C-D, and path A-E-F, the algorithm finds that the path A-C-D has the least cost; therefore it includes node D and its edge DF in the Tree. At last, comparing path A-E-F with path A-C-D-F, the least cost path from source node A to destination node F is found as A-C-D-F. Then the traffic is routed through path A-C-D-F. The algorithm continues to proceed to the next traffic demand.

5.5.2 Minimum Hop Count Path Routing Algorithm (MHP)

The proposed minimum hop count path routing algorithm is used to route each traffic demand through the corresponding minimum hop count path in order to minimize the total internal traffic load on the network. In this way, it is expected to achieve low average packet delay. The proposed minimum hop count path routing algorithm is presented as:

1. Set $\rho_{\max}$ =0.8. Route all one hop count traffics under the constraint that $\rho_i \leq \rho_{\max}$. Update traffic matrix and link utilization matrix.
2. Arrange all traffic demands in the decreasing order. If the maximum traffic demand is 0, then stop.

3. Starting from the heaviest traffic demand, find the minimum hop count path to route the traffic under the constraint that $\rho_i < \rho_{\max}$ for any link *i* on the path. If more than one minimum hop count path exists, choose the one with the minimum maximum link utilization. Because of the upper bound of link utilization, the part of traffic that can't be routed through the path remains unrouted. Update traffic matrix and link utilization matrix. If no such path exists, consider next traffic demand. Repeat Step 3 until all traffic demands are considered. Go to Step 2.

At step 3, For a path with *m* links, the maximum link utilization of the path is defined as: max { ρ_i , *i* =1, 2, … , *m*}. This concept is also used in the following two routing algorithms. By setting the cost of each link to be 1, a modified Dijkastra's algorithm is used to find the minimum hop count path for a given traffic under link utilization constraint. From source node to any intermediate node or the destination node, if two or more minimum hop count paths are found, the algorithm chooses the path with minimum maximum link utilization.

Given network topology and link utilization, here an example is given on how to find the minimum hop count path to route a given traffic. For a six nodes network of degree three shown in Figure 5.4, assume the cost of each link is 1. The current link utilizations are shown in the figure. To route a given traffic

from source node A to destination node F, the modified Dijkastra's algorithm is used to find the minimum hop count path. It operates as follows.

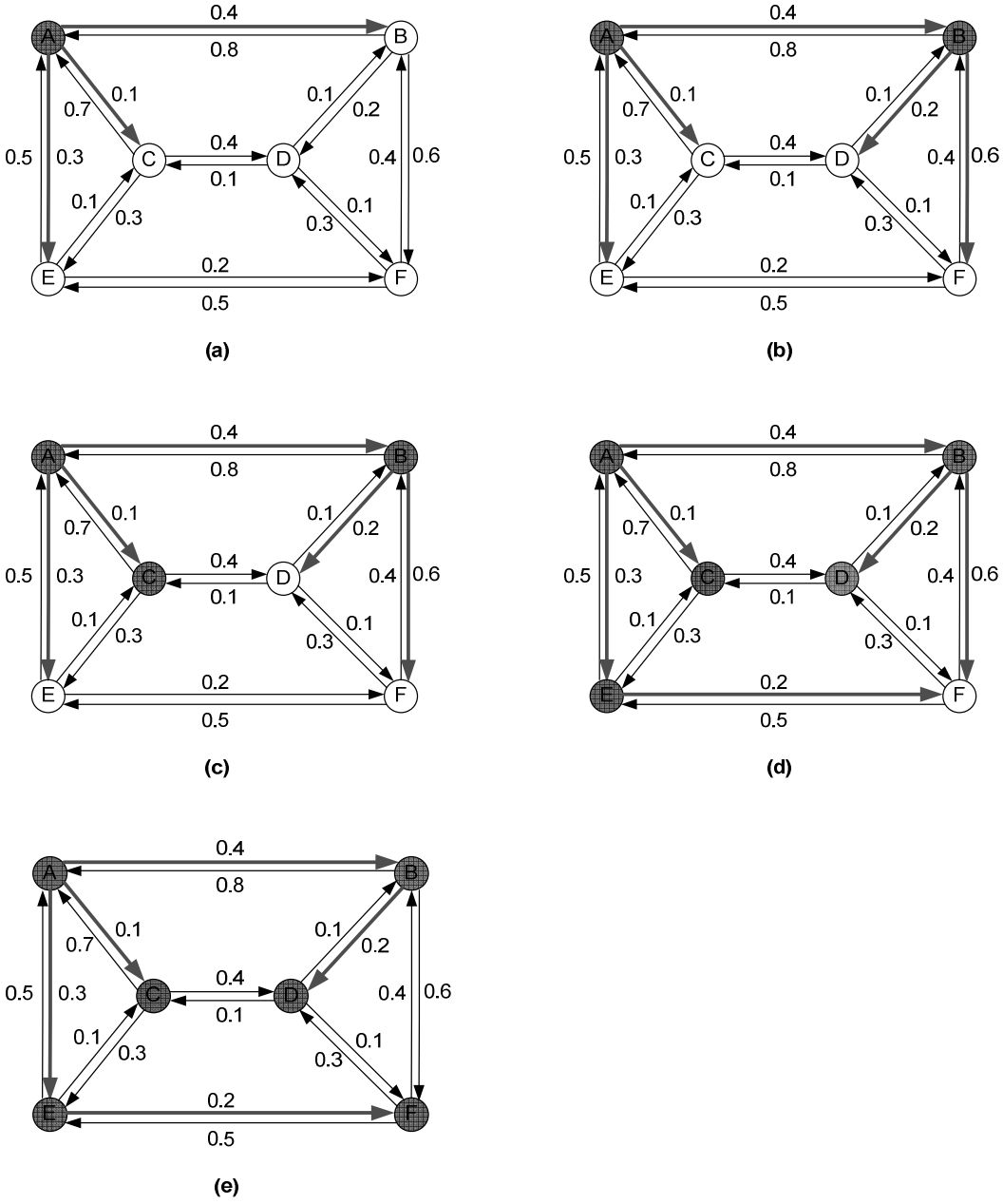

Figure 5.4 Minimum hop count path routing

First the source node A and its edges (AB, AC, AE) are included in a Tree. Since AB, AC, and AE are all one hop count path, the algorithm picks node B and its edges (BD, BF), and includes them in the Tree. At the next step, since both path A-C, and A-E have only one hop compared with path A-B-D, and A-B-F of two hops, the algorithm picks node C, and includes it and its edges (CD, CE) in the Tree. From node A to node D, the algorithm compares path A-C-D with path A-B-D. It keeps path A-B-D as the minimum hop count path from A to D. From node A to B, since path A-B has only one hop count, but path A-C-B has two hop counts, path A-B remains. From node A to E, since path A-E has one hop, path A-C-E has two hops, path A-E is kept as the minimum hop count path from node A to node E. The algorithm continues to pick up node E and its edges (EC, EF), and includes them in the Tree. Then it compares path A-C with path A-E-C, and keeps path A-C. It compares path A-B-F with path A-E-F. Both paths have the same cost (or two hop counts), but path A-B-F has the minimum maximum link utilization, therefore path A-B-F is chosen as the minimum hop count path from node A to node F. The traffic is thus routed through this path, and the algorithm continues to proceed to the next traffic demand.

5.5.3 Minimum Hop Count with Load Balancing Routing Algorithm (MHLB)

The MHLB routing algorithm is used to route all traffic based on the hop count of the paths. All one hop count traffic is routed first, then two hop count traffic, next three hop count traffic, and so on. The maximum link utilization of a link is set at 0.6 first, which is increased up to 0.8 in the subsequent rounds. The steps are as follows.

1. Set $\rho_{\max}$ =0.6. Route all one hop count traffics under the constraint that $\rho_i \leq \rho_{\max}$. Update traffic matrix and link utilization matrix. Set counter = 1.
2. Arrange all traffic demands in the decreasing order. If the maximum traffic demand is 0, then stop. Otherwise increase counter by 1 (or counter++), let $\rho_{\max} = \rho_{\max} + \alpha$, $0 < \alpha \leq 0.2$ (the actual value of α selected is determined by searching the optimal value from a small set). If $\rho_{\max}$ > 0.8, then set $\rho_{\max}$ =0.8.
3. Starting from the heaviest traffic demand, find the path with total hop count less or equal to counter to route the traffic under the constraint that $\rho_i < \rho_{\max}$ for any link *i* on the path. If more than one such path exists, choose the one with the minimum maximum link utilization.

Update traffic matrix and link utilization matrix. If no such path exists, consider next traffic demand. Repeat Step 3 until all traffic demands are considered. Go to Step 2.

At step 3, a modified Bellman-Ford algorithm is used to find the path with total hop count less or equal to counter to route a given traffic. Traffic load balancing is achieved through increasing the upper bound of link utilization from 0.6 to 0.8 step by step. The MHLB is expected to achieve low average delay, low total internal traffic, and least blocked traffic.

At step 3, the hop count constraint is set as equal to counter, and the upper bound of link utilization equals to $\rho_{\max}$. For an n node network, to route a given traffic from source node s to destination node t, the modified Bellman-Ford algorithm is stated as follows. First it defines,

w(i, j) = link cost (or weight) from node i to node j; if i = j, w(i, j)= 0; if two nodes are directly connected, and ρ(i, j) < $\rho_{\max}$, then w(i, j) = 1; otherwise, w(i, j) = ∞.

h = maximum number of links in a path at the current stage of the algorithm, h ≤ counter.

$L_h(n)$ = cost (equals to hop count from node s to n) of the least-cost path From node s to node n under the constraint of no more than h

links, $L_h(n) \leq$ counter.

$\rho_h(n)$ = the maximum link utilization of the least-cost path from node s to node n.

The modified Bellman-Ford algorithm operates according to the following two steps. Step 2 is repeated until none of the costs changes:

Step 1: $L_0(n) = \infty$, for all $n \neq s$

$L_h(s) = 0$, for all h

Step 2: For each successive $h \geq 0$, and each $n \neq s$, compute

$$L_{h+1}(n) = \min_j [L_h(j) + w(j, n)]; \quad j \text{ is the predecessor node of node n}$$

If $\rho_{h+1}(n) \leq \rho_h(n)$, then the previous path remains; otherwise, the newly find path is kept, and the old one is removed.

If h = counter, and n = t, stop; otherwise, repeat step 2.

Given network topology and link utilization information, here an example is given to show how the algorithm operates to find the path to route a given traffic. For a six nodes network of degree three shown in Figure 5.5, assume the cost of each link is 1. The current link utilization information is shown in the Figure 5.5(a). Now, suppose the amount of a given traffic from source node A to destination node F will result in an increase of link utilization by 0.6 on any link if the whole traffic is routed through that link. To route the given traffic

from source node A to destination node F, the modified Bellman-Ford algorithm operates as follows to find the path.

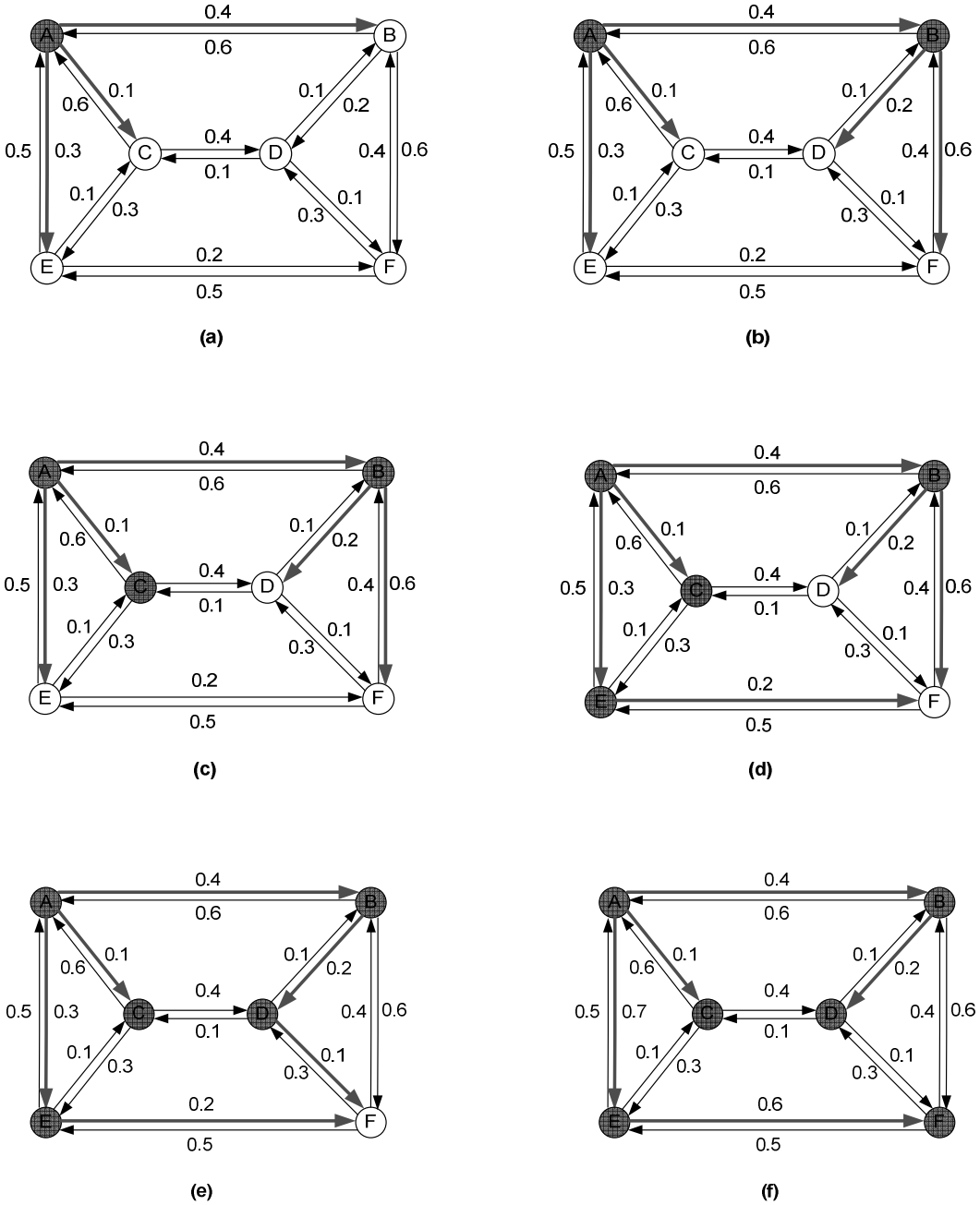

Figure 5.5 MHLB routing

Suppose at current stage, the upper bound of link utilization $\rho_{\max}$ = 0.7 and the counter equals 3, which means that the maximum hop count of the path from node A to node F shouldn't exceed 3. The algorithm first picks up source node A and one hop count path A-B, A-C, and A-E; then proceeds to two hop count paths. The algorithm picks up node B, and its edges BD and BF, and finds two hop count paths A-B-D, and A-B-F. Then it picks up node C, and its edges CD and CE, and compare path A-C-D with path A-B-D. These two paths all have two hop counts, and the same maximum link utilization, the algorithm picks path A-B-D, path A-C-D is removed. The algorithm also compares path A-C-E with path A-E. Even though both paths have the same maximum link utilization, path A-E has only one hop count, therefore path A-E remains. The algorithm continues to proceeds to pick up node E, and its edges EC and EF. It compares path A-E-C with path A-C, then it chooses path A-C. It then compares path A-E-F with path A-B-F. It chooses path A-E-F since path A-E-F has lower maximum link utilization. The algorithm proceeds to three hop count path. It picks node D and its edge DF. It compares path A-B-D-F with path A-B-F, path A-B-D-F is kept because it has lower maximum link utilization. It continues to compare path A-B-D-F with path A-E-F, then path A-E-F remains since path A-E-F has lower maximum link utilization. The algorithm stops since h = counter, and the path is found. At last, part of the traffic is routed through path A-E-F to make its maximum link utilization increase to 0.7 because 0.7 is

the current link utilization constraint. The rest of the traffic remains unrouted until next round. In this way, traffic is not only routed through paths of lower hop count, which should lead to less total internal traffic, but also distributed more evenly.

5.5.4 Minimum Hop Count Routing Algorithm (MH)

Proposed MH routing algorithm is used to route all traffic demands based on the hop count of the paths similar to MHLB. All one hop count traffic are routed first, then two hop count traffic, next three hop count traffic, and so on. However for MH algorithm, the upper bound of link utilization always remains as 0.8 during the whole process.

1. Set $\rho_{\max}$ =0.8. Route all one hop count traffic under the constraint that $\rho_i \leq \rho_{\max}$. Update traffic matrix and link utilization matrix. Set counter = 1.
2. Arrange all traffic demands in the decreasing order. If the maximum traffic demand is 0, then stop. Otherwise increase counter by 1 (or counter++).
3. Starting from the heaviest traffic demand, find the minimum hop count path with total hop count less or equal to counter to route the traffic under the constraint that $\rho_i < \rho_{\max}$ for any link *i* on the path. If more than

one such path exists, choose the one with the minimum maximum link utilization. Update traffic matrix and link utilization matrix. If no such path exists, consider next traffic demand. Repeat Step 3 until all traffic demands are considered. Go to Step 2.

At step 3, the previous modified Bellman-Ford algorithm is used to find the minimum hop count path with total hop count less or equal to counter to route a given traffic demand. Through MH routing the total internal traffic is expected to be the least. However, since the upper bound of link utilization is not increased step by step as MHLB, with MH routing, traffic is not so evenly distributed as the MHLB.

5.6 Simulations and analysis

Case1:

Assume a physical layer network topology of degree 3 with 10 nodes and 15 links. The departure rate μ is set as 130 units.

(a) Light external traffic demands:

For a 10-node network, there are 10×9 distinct source-destination node pairs. Therefore 90 external traffic demands are generated randomly from 0 to 9 units corresponding to the 90 different source-destination node pairs.

Simulations are done over 10 different topologies with proposed four different routing algorithms to route the traffic. Under light external traffic demands, the total blocked traffic is 0. The average delay is shown in Table 5.1.1.

Table 5.1.1 Average delay (ms)

Topology	LCP	MHP	MHLB	MH
1	18.64	18.62	18.62	18.62
2	21.73	21.87	21.69	21.69
3	18.66	18.64	18.61	18.61
4	19.13	19.14	19.17	19.17
5	22.76	22.79	22.8	22.8
6	22.29	22.48	22.66	22.66
7	18.6	18.58	18.61	18.61
8	18.28	18.28	18.45	18.45
9	23.19	23.19	23.19	23.19
10	21.24	21.11	21.06	21.06

(b) Heavy traffic demands:

90 external traffic demands are generated randomly from 0 to 19 units corresponding to the 90 different source-destination node pairs. Simulations are done over the same 10 different topologies with proposed four different

routing algorithms to route the traffic. The average delay under heavy traffic load is shown in Table 5.1.1. The total blocked traffic in different scenarios is shown in Table 5.1.2.

Table 5.1.2 Average delay (ms)

Topology	LCP	MHP	MHLB	MH
1	28.17	28.24	27.55	27.59
2	40.85	42.26	39.95	39.95
3	27.42	27.65	27.1	27.21
4	30.39	30.81	29.89	30.28
5	42.88	43.23	40.88	40.88
6	39.44	38.45	37.86	37.92
7	27.69	27.83	27.87	28.02
8	27.16	27.28	27.39	27.42
9	51.87	49.45	47.65	48.03
10	42.48	40.77	39.22	39.24

Table 5.1.3 Total blocked traffic (units)

Topology	LCP	MHP	MHLB	MH
1	0	0	0	0
2	25	25	25	25
3	0	0	0	0
4	0	0	0	0
5	35	35	35	35
6	32	32	32	32
7	0	0	0	0
8	0	0	0	0
9	35	35	35	35
10	14	14	14	14

Case 2:

Assume a physical layer network topology of degree 4 with 30 nodes and 60 links. The departure rate μ is set as 280 units.

(a) Light external traffic demands:

For a 30-node network, there are 30×29 distinct source-destination node pairs. Therefore 870 external traffic demands are generated randomly from 0 to 9 units corresponding to the 870 different source-destination node pairs.

Simulations are done over 10 different topologies with proposed four different routing algorithms to route the traffic. In all different scenarios, the total blocked traffic is 0. The average delay is shown in Table 5.2.1.

Table 5.2.1 Average delay (ms)

Topology	LCP	MHP	MHLB	MH
1	16.0	16.20	16.07	16.07
2	23.91	25.13	24.53	24.59
3	20.01	20.84	20.98	20.99
4	22.78	24.46	23.94	24.35
5	20.46	21.37	21.44	21.49
6	23.51	26.66	24.81	25.85
7	22.48	24.11	23.71	23.99
8	19.02	19.40	19.62	19.63
9	22.12	24.0	23.0	23.35
10	18.32	18.92	18.58	18.84

(b) Heavy external traffic demands:

870 external traffic demands are generated randomly from 0 to 10 units corresponding to the 870 different source-destination node pairs. Simulations

are done over the 10 different topologies with proposed four different routing algorithms to route the traffic. The average delay is shown in Table 5.2.2. The total blocked traffic in different scenarios is shown in Table 5.2.3.

Table 5.2.2 Average delay (ms)

Topology	LCP	MHP	MHLB	MH
1	17.35	17.61	17.37	17.37
2	24.40	25.67	24.21	24.21
3	22.86	24.10	24.08	24.31
4	26.88	29.9	28.37	28.99
5	23.44	25.05	24.86	25.12
6	27.04	33.40	29.56	31.15
7	25.48	26.87	27.50	27.02
8	21.44	22.17	22.19	22.32
9	25.88	28.08	27.06	27.65
10	20.19	21.04	20.58	21.02

Table 5.2.3 Total blocked traffic (units)

Topology	LCP	MHP	MHLB	MH
1	0	0	0	0
2	154	154	154	154
3	0	0	0	0
4	0	0	0	0
5	0	0	0	0
6	0	0	0	0
7	44	83	14	49
8	0	0	0	0
9	0	0	0	0
10	0	0	0	0

The proposed three new routing algorithms are compared against the LCP algorithm, which is based on routing that mathematically minimizes the end-to-end delay. The LCP algorithm routes as much as possible traffic through the least cost path until the maximum link utilization 0.8 is reached. Because of this reason, LCP does not, under heavy traffic load, distribute traffic evenly over all available paths. Since the proposed MHLB algorithm does distribute

the traffic more evenly by setting at first a link utilization limit of 0.6, and then increasing it up to 0.8 if necessary, MHLB is expected to result in better performance than LCP in most cases. Note also that while LCP determines the route after a computationally intensive process, MHLB doesn't require the computation of link cost prior to determining the route. It simply routes the traffic based on the hop count of the path, subject to, the limits on link utilization. Further, for the LCP algorithm, the link cost depends on the traffic, and the traffic in turn depends on the routes chosen. Because of the existence of this feedback condition, instabilities may result.

Simulation results show that for the small sized FSO networks, under light traffic demands, the performance of the three proposed algorithms are similar to each other; under heavy traffic load, the proposed MHLB routing algorithm results in minimum average delay. For large sized FSO networks, simulation results show that, under light traffic demands, MHLB results in minimum average delay in most cases; under heavy traffic load, it results in minimum average delay and least blocked traffic in most cases. Compared with LCP, MHLB performs better for small sized FSO networks. For large sized FSO networks, even though LCP results in less average delay than MHLB, MHLB is expected to outperform LCP with the increase of the nodal degree because of its traffic load balancing feature.

5.7 Summary

This chapter has proposed and analyzed four routing algorithms for degree-constrained FSO mesh networks of different sizes under varying traffic demands. In each case, the cost is characterized by average delay. The maximum link utilization is set as 0.8. Traffic that exceeds this constraint is regarded as blocked traffic. Simulation results show that for small sized FSO networks, under light traffic demands, the performance of the three proposed algorithms are similar to each other; under heavy traffic load, the proposed MHLB routing algorithm outperforms the others in most cases. For large sized FSO networks, simulation results show that MHLB performs best in most case.

Chapter 6

Conclusions

Abstract: This dissertation has considered the physical topology design and routing problems in degree constrained free-space optical mesh networks. It has devised and presented a physical topology design scheme that improves the reliability of FSO networks such that the atmospheric effects and other environmental effects on FSO networks could be mitigated. Further, it has researched and presented four different routing algorithms that address the routing issues specific to packet switched FSO mesh networks. Based on the parameters of performance, the dissertation has recommended a specific routing algorithm that minimizes the mean delay while distributing the traffic load more evenly in the network. The results are based on extensive simulations involving a large number of topologies, varying degrees of the FSO nodes, and varying traffic loads.

6.1 Achievements

It has been shown through research conducted by various researchers that the performance of an FSO system can be affected by various factors, especially environmental factors. Chapter 3 has proposed an angle

enlargement scheme between adjacent FSO links at an FSO node in order to mitigate the environmental effects. This work involved using the properties of a basic structure in computational geometry called Delaunay Triangulation. In this approach, first the Delaunay Triangulation of a given point (or FSO node) set is formed, and then edges (or FSO links) are removed from the DT graph in order to satisfy the degree constraint of the FSO network. This dissertation has augmented the process for the specific case of FSO mesh networks. As a result, in a network constructed with the use of the proposed NTD algorithm, the minimum angle at each node is enlarged leading to enhanced reliability of the FSO network. Simulations show that FSO networks constructed with the NTD algorithm achieve not only high spatial diversity, but also high reliability. Further, the proposed NTD algorithm also results in higher link connectivity, node connectivity, and lower minimum hop count between the source and destination nodes. Chapter 4 extends the NTD algorithm to the 3-dimensional space, thus increasing the application space of the algorithm.

To solve the routing problem in packet switching FSO mesh networks, four different routing algorithms have been proposed and their performances evaluated through simulations for a number of FSO mesh networks with different topologies, nodal degrees, and varying intensities of traffic. The proposed least cost path (LCP) routing algorithm, which is based on

minimizing the end-to-end delay, has been considered as the bench mark. The performance of each of the other three proposed algorithms was evaluated against the bench mark. The proposed minimum hop count with load-balancing (MHLB) routing algorithm, while being computationally tractable, has been recommended as the algorithm of choice because it performs best in most cases compared with the other two. It results in the minimum average delay; least blocked traffic, and balanced load distribution.

6.2 Future work

Based on what have been presented in this dissertation, future work may focus on two areas: security in FSO networks, and mobile FSO networks.

Previous research on the security of fiber optical networks, especially security in Ethernet passive optical networks (EPON), has been published in [99]. However, FSO networks bring a different set of challenges as far as their security is concerned. This topic has not been explored at this point. Compared with RF wireless technology, FSO is a much more secure wireless technology. First, since FSO laser beams are immune to electromagnetic interference, they are hard to detect, and hard to jam. Second, since FSO links are directional point-to-point laser beams, it can't be intercepted easily. However, it states in [100] that "in certain circumstances unauthorized access

is still possible, due to the fact, that part of the communication beam radiation is reflected and/or scattered by solid objects within the beam, dust and/or water droplets on window panes, and particles of atmospheric aerosol. If the wavelength is known a priory, and if specially designed equipment is used, detection and eavesdropping may be implemented under some specific conditions at distances up to several hundred meters." Future work in FSO network security will likely focus in this area.

Currently, mobile FSO technology is still in its infancy [101]. Few publications can be found on mobile FSO networks. Reference [101] discusses critical technology, integration, and network architecture gaps as well as the potential approaches for implementing mobile FSO networks. Reference [102] presents a brief overview of several demonstrations of mobile FSO systems, and discusses error correction and retransmission techniques for mobile FSO transmission. Reference [103] investigates the challenge caused by beam divergence and optical power level in mobile FSO communications, and presents an analytical model of the receiver beam profile of a mobile FSO link. More works need to be done in the area of mobile FSO networks. This will be specifically in the area of alignment and tracking while in a state of mobility. Battlefield applications of this technology will further require a robust secure framework.

References

1. *Free-space laser communications : principles and advances* ed. A.K. Majumdar and J.C. Riclkin. 2007: Springer.

2. Bouchet, O., et al., *Free-space optics: propagation and communication*. 2006: Wiley-ISTE.

3. Willebrand, H. and B. Ghuman, *Free space optics : enabling optical connectivity in today's networks*. 2002.

4. Schuster, J. *Free Space Optics (FSO) Technology Overview*. 2002 http://www.fcc.gov/realaudio/presentations/2002/100302/technology_overview.ppt.

5. Shaulov, G., et al., *Simulation-assisted design of free space optical transmission systems*, in *IEEE Military Communication Conference*. 2005. p. 1-5.

6. Muhammad, S.S., et al., *Terrestrial free-space optical links for high bandwidth connectivity*, in *IEEE 9th International Multitopic Conference*. 2005.

7. Andrews, L.C., *Laser beam propagation through random media* Bellingham, WA: SPIE Optical Engineering Press.

8. Bloom, S., et al., *Understanding the performance of free-space optics.* Journal of Optical Networking, Optical Society of America, 2003. **VOL. 2**(No. 6): p. 178-200.

9. Kamran, K., *Performance of APD-based, PPM free-space optical communication systems in atmospheric turbulence.* IEEE Transactions on Communications, 2005. **53**(9): p. 1455 -1461.

10. Muhammad, S.S., et al., *Reed Solomon coded PPM for Terrestrial FSO Links*, in *IEEE, International Conference on Electrical Engineering*. 2007. p. 1-5.

11. Gappmair, W., Muhammad, and S.S., *Error performance of terrestrial FSO links modelled as PPM/Poisson channels in turbulent atmosphere.* Electronics Letters, 2007. **43**(5): p. 63-64.

12. Gagliardi, R.M. and S. Karp, *Optical Communications*. 2nd ed. Wiley Series in Telecommunications. 1995.

13. http://www4.ncsu.edu/~arattari/opticspaper.pdf.

14. Rabinovich, W.S., et al., *Free-space optical communications link at 1550nm using multiple-quantum-well modulating retroreflectors in a marine environment.* SPIE Optical Engineering, May 2005. **44**(5).

15. http://www.canon.com/bctv/index.html.

16. http://firstcomm.ca/pdf/PICO%20Plus%20Data%20Sheet.pdf.

17. http://www.teraoptic.com/.

18. http://www.lightpointe.com/products/default.cfm.

19. http://www.clearmesh.com/.

20. Yoshida, K. and T. Tsujimura, *Tracking control of the mobile terminal in an active free-space optical communication system*, in *SICE-ICASE International Joint Conference*. 2006.

21. Dwivedi, A., *Critical technology gaps and potential solutions for mobile free space optical networking*, in *IEEE Military Communications Conference*. 2006.

22. Willebrand, H.A. and B.S. Ghuman, *Fiber optics without fiber.* IEEE Spectrum, Aug. 2001. **38**(8): p. 40-45.

23. http://www.freespaceoptics.org/freespaceoptics/topologies/default.cfm.

24. http://en.wikipedia.org/wiki/Network_topology.

25. http://fallsconnect.com/topology.htm.

26. Chen, Y.-C., C.-C. Sue, and S.-Y. Kuo, *The Survivability of the Augmented Logical Ring Topology in WDM Networks*, in *IEEE 12th Pacific Rim International Symposium on Dependable Computing*. Dec. 2006. p. 397-398.

27. Yoon, G., et al., *Ring Topology-based Redundancy Ethernet for Industrial Network*, in *SICE-ICASE, 2006. International Joint Conference*. Oct. 2006. p. 1404-1407.

28. Shalom, M., P.W.H. Wong, and S. Zaks, *Optimal On-Line Colorings for Minimizing the Number of ADMs in Optical Networks*, in *9th International Conference on Transparent Optical Networks, ICTON '07.* . July 2007. p. 58 - 58.

29. Prytz, G., *Network recovery time measurements of RSTP in an ethernet ring topology*, in *IEEE Conference on Emerging Technologies & Factory Automation, 2007. ETFA.* . Sept. 2007. p. 1247 - 1253.

30. Oh, J.-t., D.-Y. Kim, and H.-J. Kim. *A design of the OAM flow in the ring topology ATM networks*. in *IEEE International Conference on Communication Technology Proceedings*. May 1996.

31. Dao, H.M. and C.B. Silio, Jr., *Ring-network with a constrained number of consecutively-bypassed stations.* IEEE Transactions on Reliability, March 1998. **47**(1): p. 35 - 43.

32. Wang, X., T. Ahonen, and J. Nurmi, *Applying CDMA Technique to Network-on-Chip.* IEEE Transactions on Very Large Scale Integration (VLSI) Systems, Oct. 2007. **15**(10): p. 1091 - 1100

33. Lian, Z., et al., *Resilient ethernet ring for metropolitan area networks*, in *The Ninth International Conference on Communications Systems, 2004. ICCS 2004.* . Sept. 2004. p. 316 - 320.

34. Desai, A. and S. Milner, *Autonomous reconfiguration in free-space optical sensor networks.* IEEE Journal of Selected Areas in Communications, 2005. **VOL. 23**(NO. 8): p. 1556-1563.

35. Kamal, A.E., *A discrete-time approach to the modeling of carrier-sense multiple-access on the bus topology.* IEEE Transactions on Communications, 1992. **40**(3): p. 533 - 540

36. Kuroyanagi, N., *Adaptive and portable TDMA LAN with a bus topology*, in *IEEE Global Telecommunications Conference, GLOBECOM '88.* 1988. p. 1808 - 1812.

37. Kamal, A.E., *Analysis of the semisynchronous carrier sense multiple access on the bus topology.* IEEE Transactions on Communications, 1993. **41**(11): p. 1635 - 1646.

38. Chapman, D.A., P.A. Davies, and J. Monk, *Code-division multiple-access in an optical fiber LAN with amplified bus topology: the SLIM bus.* IEEE Transactions on Communications, Sept. 2002. **50**(9): p. 1405 - 1408.

39. Li, D., P.H. Chou, and N. Bagherzadeh. *Topology selection for energy minimization in embedded networks*. in *Proceedings of the Asia and South Pacific-Design Automation Conference*. 2003.

40. Vukovic, I.N. and K.S. Vastola, *An analysis of a new carrier sensing scheme for undirectional bus CSMA networks*, in *1996 IEEE International Conference on Communications*. 1996. p. 1088 - 1092.

41. Irshid, M.I. and M. Kavehrad, *A WDM cross-connected star topology for multihop lightwave networks.* Journal of Lightwave Technology, 1992. **10**(6): p. 828 - 835.

42. Barranco, M., et al., *An active star topology for improving fault confinement in CAN networks.* IEEE Transactions on Industrial Informatics, May 2006. **2**(2): p. 78 - 85.

43. Barranco, M., L. Almeida, and J. Proenza, *ReCANcentrate: a replicated star topology for CAN networks*, in *10th IEEE Conference on Emerging Technologies and Factory Automation*. Sept. 2005. p. 8.

44. Chang, M.-S., et al. *The distributed program reliability analysis on star topologies*. in *1998 International Conference on Parallel and Distributed Systems*. 1998.

45. Sarac, K. and K.C. Almeroth, *Tracetree: a scalable mechanism to discover multicast tree topologies in the Internet.* IEEE/ACM Transactions on Networking, Oct. 2004. **12**(5): p. 795 - 808.

46. Patarasuk, P. and X. Yuan. *Bandwidth Efficient All-reduce Operation on Tree Topologies*. in *Parallel and Distributed Processing Symposium, IEEE International*. March 2007.

47. Datta, R., et al., *An algorithm for optimal assignment of a wavelength in a tree topology and its application in WDM networks.* IEEE Journal on Selected Areas in Communications, Nov. 2004. **22**(9): p. 1589 - 1600.

48. Stallings, W., *High-Speed Networks and Internet: Performance and Quality of Service*. 2nd ed. 2002, New Jersy: Prentice Hall.

49. Cahn, R.S., *Wide area network design: concepts and tools for optimization*. Morgan Kaufmann Series in Networking. 1998.

50. Tanenbaum, A.S., *Computer Networks*. 4th ed. 2002: Prentice Hall.

51. Saab, Y. and M. VanPutte, *Shortest path planning on topographical maps.* IEEE Transactions on Systems, Man and Cybernetics, Part A,, Jan. 1999. **29**(1): p. 139 - 150.

52. Lee, D.C., *Proof of a modified Dijkstra's algorithm for computing shortest bundle delay in networks with deterministically time-varying links.* IEEE Communication Letters, Oct. 2006. **10**(10): p. 734 - 736.

53. Djukic, P. and S. Valaee, *Link Scheduling for Minimum Delay in Spatial Re-Use TDMA*, in *26th IEEE International Conference on Computer Communications, INFOCOM 2007.* . May 2007. p. 28 - 36.

54. Kartalopoulos, S.V., *Free Space Optical Mesh Networks For Broadband Inner-city Communications* in *NOC 2005,10th European Conference on Networks and Optical Communications*. July, 2005: University College London. p. 344-351.

55. Kartalopoulos, S.V., *Free Space Optical Nodes Applicable to Simultaneous Ring &Mesh Networks* in *Proceedings of the SPIE European Symposium on Optics & Photonics in Security & Defense*. Sep. 2006: Sweden.

56. Chadha, D., *Feasibilty Study of Free Space Optical Communication Link Through Atmospheric Turbulent Channel*, in *IEEE conference on optoelectronic and microelectronic meterials and devices*. Dec. 2004. p. 311-314.

57. Erich Leitgeb, S.S.M., Christoph Chlestil, Michael Gebhart, Ulla Birnbacher. *Reliability of FSO links in next generation optical networks*. in *7th International Conference on Transparent Optical Networks*. IEEE Proc. of 2005.

58. Zhuanhong Jia, Q.Z., and Faliang Ao. *Atmospheric attenuation analysis in the FSO link*. in *International Conference on Communication Technology, IEEE*. 2006.

59. Tsiftsis, T.A., et al., *Multihop free-space optical communications over strong turbulence channels*, in *IEEE International Conference on Communications*. ICC2006. p. 2755-2759.

60. Minch, J.R., D.R. Gervais, and D.J. Townsend, *Adaptive transceivers for mobile free-space optical communications*, in *IEEE Military Communications Conference*. MILCOM 2006.

61. Abtahi, M., et al., *Suppression of turbulence-induced scintillation in free-space optical communication systems using saturated optical amplifiers.* Journal of Lightwave Technology, 2006. **Vol. 24**(No. 12): p. 4966-4973.

62. Haiping Wu, B.H., and Mohsen Kavehrad, ",", 2004. , . *Achieving carrier class availability of FSO link via a complementary RF link*, in *IEEE Conference record of the Thirty-eighth Asilomar Conference on Signals, Systems and Computers*. 2004. p. 1483-1487.

63. Akella, J., M. Yuksel, and S. Kalyanaraman, *Error analysis of multi-hop free-space optical communication*, in *IEEE International Conference on Communications*. ICC2005. p. 1777-1781.

64. Liorca, J., A. Desai, and S. Milner, *Obscuration minimization in dynamic free space optical networks through topology control*, in *IEEE Military Communications Conference* 2004.

65. Zhuang, J., M.J. Casey, and S.D. Milner, *Multi-objective optimization techniques in topology control of free space optical networks*, in *IEEE Milittary Communications Conference* 2004.

66. Hu, L., *Topology control for multihop packet radio networks.* IEEE Transactions on Communications, 1993. **VOL. 41**(NO. 10): p. 1474-1481.

67. Fang Liu, U.V., and Stuart Milner, *Bootstrapping free-space optical networks.* IEEE Journal on Selected Areas in Communications, 2006. **Vol. 24**(No.12): p. 13-22.

68. Gurumohan, P.C. and J. Hui. *Topology design for free space optical networks*. in *Proc. Of IEEE Computer Communications and Networks*. 2003.

69. Berg, M.d., et al., *Computational Geometry: Algorithms and Applications*. 1997: Springer.

70. Hu, L., *Distributed algorithms for multihop packet radio networks*. 1990, UC: Berkeley.

71. Megerian, S., et al., *Worst and Best-Case Coverage in Sensor Networks.* IEEE Transactions on Mobile Computing, 2005. **4**(1): p. 84-92.

72. Wu, C.-H., K.-C. Lee, and Y.-C. Chung, *A Delaunay triangulation based method for wireless sensor network deployment*, in *IEEE 12th International Conference on Parallel and Distributed Systems*. 2006.

73. Li, Y.-Y., et al., *Localized Delaunay Triangulation with Application in Ad Hoc Wireless Networks.* IEEE Transactions on Parallel and Distributed Systems, Oct. 2003. **14**(No.10): p. 1035-1047.

74. Liebeherr, J., M. Nahas, and W. Si, *Application-layer multicasting with Delaunay triangulation overlays.* IEEE Journal on Selected Areas in Communications, Oct. 2002. **20**(8): p. 1472-1488.

75. Spelic, D., F. Novac, and B. Zalik, *Delaunay Triangulation Benchmarks.* Journal of ELECTRICAL ENGINEERING, 2008. **59**(1): p. 49-52.

76. Meguerdichian, S., et al., *Exposure In Wireless Ad-Hoc Sensor Networks.* ACM SIGMOBILE, 2001: p. 139-150.

77. Park, D.G., H.G. Cho, and Y.S. Kim, *A TIN Compression Method using Delaunay Triangulation.* International Journal of Geographical Information Science (IJGIS), 2001. **15**(3): p. 255-269.

78. Plantier, J., L. Boutt'E, and S. Lelandais, *Defect Detection on Inclined Textured Planes Using the Shape from Texture Method and the Delaunay Triangulation.* EURASIP Journal on Applied Signal Processing, 2002(No. 7): p. 659-666.

79. Narula, S.C. and C.A. Ho, *Degree-constrained minimum spanning tree.* Comput. & Ops. Res., 1980. **Vol. 7**: p. 239-249.

80. C., M.G., P.M. Resende, and Pardalos, *Handbook of optimization in telecommunications*. 2006: Springer.

81. Bollobas, B., *Modern graph theory*. 1998: Springer.

82. *Omnilux Mesh Network Installation Manual V3.0*. 2006.

83. Aurenhammer, F., *Voronoi Diagrams - A Survey of Fundamental Geometric Data Structure.* ACM Computing Surveys, 1991. **23**(3).

84. Fang, J., *Sweepline Algorithm for Unstructured Grid Generation*. 1991, The University of Texas at Arlington.

85. A. R. Mohd Shariff and M.E. Woodward, *A Delay Constrained Minimum Hop Distributed Routing Algorithm using Adaptive Path Prediction.* Journal of Networks, 2007. **Vol.2**(No.3): p. 46-57.

86. Bhandari, R. *Optimal diverse routing in Telecommunication Fiber Networks*. in *Proc. of the 13th IEEE INFOCOM conference on networking for global communications*. 1994. Toronto.

87. R. Guerin and A. Orda, *Computing shortest paths for any number of hops.* IEEE/ACM Trans. on Networking, 2002. **Vol.10**: p. 613-620.

88. Cheng, G. and N. Ansari, *Finding All Hops Shortest Paths.* IEEE Communication Letters, 2004. **Vol.8**(No.2): p. 122-124.

89. Ayoub, J.N. and B.M. AI-Ramadna. *Average network delay in packet switched networks*. in *Proc. of ICECS '99. The 6th international conference on electronics, circuits and systems*. 1999.

90. Leung, K.-C. and V.O.K. Li, *Generalized Load Sharing for Packet-Switching Networks I: Theory and Packet-Based Algorithm.* IEEE Transactions on Parallel and Distributed Systems, 2006. **17**(No. 7): p. 694-702.

91. Leung, K.-C. and V.O.K. Li, *Generalized Load Sharing for Packet-Switching Networks II: Flow-Based Algorithms.* IEEE Transactions on Parallel and Distributed Systems, 2006. **17**(No. 7): p. 703-711.

92. *Inverse Multiplexing for ATM (IMA) Specification Version 1.1*, in *ATM Forum Technical Committee*. Mar. 1999.

93. Bak, S., et al. *Load-balanced Routing and Scheduling for Real-Time Traffic in Packet-Switch Networks*. in *25th Annual IEEE International Conference on Local Computer Networks*. 2000.

94. Curado, M. and E. Monteiro. *A Survey of QoS Routing Algorithms*. in *Proc. of the International conference on Information Technology*. 2004.

95. Lee, K. and K. Kim, *Dynamic Topology Control and Routing in Wireless Ad Hoc Networks.* IEICE Trans. on INF. & SYST., 2006. **Vol.E89-D**(No.5): p. 1672-1675.

96. Hu, Z., P. Verma, and J. James Sluss, *Improved Reliability of Free-space Optical Mesh Networks Through Topology Design.* Journal of Optical Networking, Optical Society of America, 2008. **Vol.7**(5): p. 436-448.

97. Kleinrock, L., *Queueing systems.Volume II. Computer Applications*. 1976, New York: Wiley.

98. Kleinrock, L., *Communication Nets: stochastic message flow and delay*. 1972, New York: Dover Publications, INC.

99. Hu, Z., S.V. Kartalopoulos, and P.K. Verma, *RC4-based Security in Ethernet Passive Optical Networks*, in *IEEE Global Telecommunications Conference, 2006. GLOBECOM '06.* Nov. 2006. p. 1-3.

100. Vladimir, S., *Optical counter-measures and security of free-space optical communication links.* proceedings of SPIE, 2004. **5614**: p. 97-108.

101. Dwivedi, A., *Critical Technology Gaps and Potential Solutions for Mobile Free Space Optical Networking*, in *IEEE Military Communications Conference*. 2006. p. 1-7.

102. Henniger, H., B. Epple, and D. Giggenbach, *Mobil FSO Activities in Europe and Fading Mitigation Approaches*, in *17th International Conference on Radioelektronika*. 2007. p. 1-6.

103. Harris, A. and T. Giuma, *Divergence and Power Variations in Mobile Free-Space Optical Communications*, in *Third International Conference on Systems*. 2008. p. 174 - 178

Appendix

List of Publications

1. Ziping Hu, Pramode K. Verma, James Sluss Jr., “Routing in Degree-constrained FSO Mesh Networks”, accepted, will be included in *Proceedings of The 2nd International Conference on Future Generation Communication and Networking (FGCN2008)*, IEEE Computer Society, 2008.

2. Ziping Hu, Pramode K. Verma, James Sluss Jr., “Improved Reliability of FSO Mesh Networks through Topology Design”, *Journal of Optical Networking*, Optical Society of America, Vol. 7, Iss.5, pp. 436-448, 2008.

3. Ziping Hu, Stamatios V. Kartalopoulos, Pramode K. Verma, “RC4-based Security in Ethernet Passive Optical Network”, *Proceedings of IEEE Global Telecommunications Conference (GLOBECOM)*, pp.1-3, Nov. 2006.

4. Ziping Hu, Stamatios V. Kartalopoulos, “The FBG reflector method and its applicability in pre- and post-dispersion compensation models”, *WSEAS Transactions on Communications*, Vol. 4, Iss. 10, pp. 1146-1153, Oct. 2005.

5. Ziping Hu and S.V. Kartalopoulos, “Simulation Models and Evaluation of Pre- and Post-Dispersion Compensation DWDM Links Using Bidirectional DCF with FBG Reflectors”, *Proceedings of the 9th WSEAS CSCC Multiconference: Communications’05*, Athens, Greece, July, 2005.

Paper under Review

1. Ziping Hu, Pramode K. Verma, Stamatios V. Kartalopoulos, "Physical topology design for FSO mesh networks in 3-dimensional space", submitted to *SPIE Optical Engineering*, Nov. 2008.